



Composition and temporal variability of particle fluxes in an insular canyon of the northwestern Mediterranean Sea



Jordi Grinyó*, Enrique Isla, Laura Peral, Josep-Maria Gili

Institut de Ciències del Mar (ICM-CSIC), Pg. Marítim de la Barceloneta 37-49, 08003 Barcelona, Spain

ARTICLE INFO

Keywords:

Submarine canyon
Mooring lines
Settling particles
Time series
Geochemical analysis
Macroscopic components

ABSTRACT

Particle fluxes have been widely studied in canyons located in continental margins; conversely, particle fluxes in canyons in sediment starved margins incising small island margins have received very little attention and remain poorly understood. The Menorca Canyon is the largest canyon system in the Balearic Archipelago. Despite the high oligotrophic conditions of the Balearic Archipelago the canyon and surrounding areas host diverse communities dominated by benthic suspension feeders. Understanding the magnitude and variability of environmental factors influencing these communities thus remain crucial. In order to characterize the temporal variability of particle fluxes, analyze its geochemical and macroscopic composition and identify the main processes that modulate particle fluxes in the Menorca Canyon, one instrumented line with a sediment trap and a current meter was deployed at 430 m water depth from September 2010 to October 2012. Particle fluxes ranged between 190 and 2300 mg m² d⁻¹ being one of the lowest ever registered in a Mediterranean submarine canyon's head. The CaCO₃ fraction was the major constituent contrasting with the general trend observed in other Mediterranean canyons. Macroscopic constituents (fecal pellets, *Posidonia oceanica* detritus and pelagic and benthic foraminifera) presented a wide variability throughout the sampling period and were not significantly correlated with the total mass flux. The low magnitude of the registered fluxes and the lack of correlation with the observed environmental variables (e.g., currents, winds, wave height, chlorophyll-*a* biomass) suggest that there is no evident controlling mechanism. However, we could infer that resuspension processes and the presence of different hydrodynamic features (e.g., eddies, interchange of water masses) condition the magnitude and composition of particle fluxes.

1. Introduction

Continental and insular margins receive particulate matter derived from fluvial discharges (Syvitski and Morehead, 1999; Kineke et al., 2000) that can result in high sediment accumulation (Sanchez-Cabeza et al., 1999). Most of these margins are incised by submarine canyons (Harris and Whiteway, 2011) that act as conduits of sediments and organic matter from the continental shelf to deeper environments (Mullenbach et al., 2004; Lopez-Fernandez et al., 2013a). In this regard, particle fluxes within submarine canyons can be orders of magnitude larger than those registered over adjacent continental slopes (Martín et al., 2006; Zúñiga et al., 2009; Pasqual et al., 2013). The magnitude, composition and temporal variability of particle fluxes in submarine canyons are influenced by a wide range of environmental and biological factors (e.g. Lopez-Fernandez et al., 2013a; Puig et al., 2014). Hydrodynamic and meteorological mechanisms, such as river flooding, storms, or cascading events can punctually increase particle fluxes in submarine canyons through resuspension and gravity-driven processes

over short periods of time (e.g. Puig et al., 2004, 2014; Ross et al., 2009; Heussner et al., 2006). Oceanographic processes such as eddies, tidal currents, or internal waves have also been associated with increments in downward particle fluxes as they alter bottom currents causing sediment resuspension (e.g. Quaresma et al., 2007; Ross et al., 2009; Schmidt et al., 2014).

Downward particle fluxes and the main mechanisms controlling them have been widely studied in submarine canyons associated to continental landmasses (e.g. Shepard et al., 1974; Xu et al., 2002; Khripounoff et al., 2003) and large islands with high mountain ranges (≥ 2000 m) and permanent rivers systems that provide large terrestrial inputs (e.g. Kineke et al., 2000; Liu et al., 2002). However, particle fluxes in canyons located in sediment starved margins incising small island margins still remain widely unknown.

In the Mediterranean, this situation is rather surprising due to the elevated number of islands found in this basin (~200), many of which incised by submarine canyons (e.g. Acosta et al., 2002; Favalli et al., 2005; Hasiotis et al., 2007; Romagnoli et al., 2009; Sakellariou et al.,

* Corresponding author.

E-mail addresses: grinyo@icm.csic.es, jordigrinyo85@gmail.com (J. Grinyó).

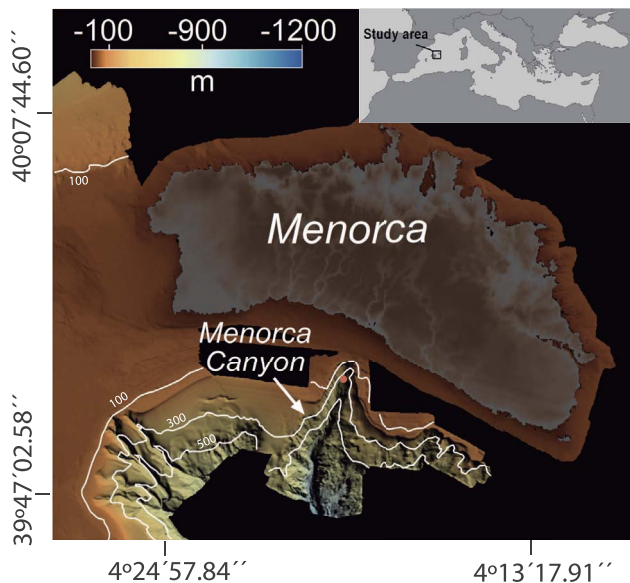


Fig. 1. Bathymetry of the southern slope of Menorca and its position in the western Mediterranean Sea, red dot indicates the location of the mooring array (Lo Iacono et al., 2014). (For interpretation of the references to colour in this figure legend, the reader is referred to the web version of this article.)

2015; Casalbone et al., 2016). Despite the relative abundance of Mediterranean insular canyons, most studies concerning downward particle fluxes in this basin have been conducted in less than 25 canyons located in the European margin. Moreover, most of these canyons incise river-dominated shelves (e.g. Bonnin et al., 2008) with higher productivity relative to the Mediterranean average (Bosc et al., 2004). The Balearic Archipelago is one of the most oligotrophic environments in the Western Mediterranean Sea (Bosc et al., 2004). In this archipelago the Menorca Canyon is the largest canyon and is located in the southern slope of Menorca Island (Fig. 1). Despite the high oligotrophy of the Balearic Archipelago, the Menorca Canyon and adjacent shelf edges and slopes hosts dense and highly diverse megabenthic assemblages characterized by a wide diversity of suspension feeders (Grinyó, 2016). To characterize the seasonal trends and magnitude of particle fluxes and environmental variables influencing megabenthic communities in the shelf edge and upper slope of the Menorca Canyon a mooring array was maintained for two years in the Menorca Canyon's head.

In this sense, the aims of this study were to characterize (1) the temporal (interannual) variability of downward particle fluxes analysing its geochemical and (2) macroscopic composition, (3) identify the main processes that modulate particle fluxes in the Menorca Canyon, and (4) set the present results within a Mediterranean context.

2. Regional setting

The Menorca Canyon is well incised in the continental shelf and slope in the southwestern margin of Menorca Island (Fig. 1) and is the largest submarine canyon system in the Balearic Archipelago.

The canyon's head is at approximately 80 m water depth and is less than 5 km off Menorca's coastline (Acosta et al., 1991). The flanks at the canyon's head are characterized by vertical walls and steep escarpments up to 20 m height (Lo Iacono et al., 2014). The continental shelf surrounding the canyon is relatively narrow and it only extends few kilometers (3–6 km) (Alonso et al., 1988). In the Menorca Canyon's head sediment creeping and cone-shaped “sediment collectors” with feeder channels have been observed with side scan sonar, demonstrating that sediment transfer from the inner shelf to the deep basins is an active process (Acosta et al., 2002). In this regard the Menorca canyon is the only canyon system in the archipelago that transports sediment to the deep basin in a confined manner (Acosta et al., 2002).

The canyon's axis presents several changes in direction. Between 80 and 1000 m depth the canyon axis presents a NNE–SSW orientation; between 1000 and 1200 m depth it presents a N–S orientation; from 1200 to 1400 m it is orientated NW–SE (Acosta et al., 2002). Finally, the canyon axis turns N–S at about 2400 m depth, where it turns into a channel with a U section (Acosta et al., 2002), which ends at the Menorca Fan a deep-sea depocenter derived from the canyon's sediment draining (Acosta et al., 2001).

The southern flank of Menorca Island is characterized by Neogene sedimentary rocks with high carbonate contents (Obrador et al., 1992). Sediment composition in the canyon and the adjacent shelves is characterized by biogenic sands with carbonate contents higher than 65% (Alonso et al., 1988). The lack of permanent river systems in the southern flank of Menorca, that deliver sediments in the adjacent coast and shelf, allow characterizing the southern margin of Menorca as a sediment starved margin (Lo Iacono et al., 2014).

The Balearic archipelago separates the Balearic-subbasin in the north from the Algerian-subbasin in the south (Amores and Monserrat, 2014) in such a way that different hydrodynamic processes and water masses influence the northern and southern slopes of the archipelago (Balbín et al., 2014). The northern slope is influenced by the Balearic current (Balbín et al., 2012; Amores et al., 2014) and is mostly characterized by the presence of resident Atlantic water (AW) (Salinity > 37.5) (Balbín et al., 2014). Conversely, the southern slope is influenced by the sporadic arrivals of mesoscale structures detached from the Algerian current and from the instability of the Almería-Oran front (Millot, 1987), which is characterized by the presence of recent AW (Salinity < 37.5) (Balbín et al., 2014). During spring and summer, when western intermediate water (WIW) is present in the Ibiza and Mallorca channel, a density front that separates the resident AW from the recent AW develops south of the archipelago (Balbín et al., 2014). Under these conditions anticyclonic gyres have been detected in the southern slope of the Menorca Island (García et al., 2005; Balbín et al., 2014). Waters surrounding the archipelago are considered oligotrophic (Fernández de Puelles et al., 2007) as they receive little quantities of nutrients from land runoff due to low precipitation and the absence of rivers (Estrada, 1996). In some areas of the archipelago these conditions are enhanced by the intrusion of nutrient-poor recent AW including the southern slope of Menorca Island (García et al., 2005).

3. Material and methods

3.1. Field work and instrumentation

One mooring array was maintained for two consecutive years in the Menorca canyon's head (39°50.6601'N, 004°01.2600'E) at approximately 430 m water depth. The mooring array was equipped with one cylindrical sediment trap Technicap PPS3 and a Aanderaa current meter RCM9, tethered 30 m above the seabed and 25 m above the seabed, respectively. The sediment trap was set with 24 sequential collecting cups filled with a buffered 5% formaldehyde solution. The first sampling period (T1) continuously operated for 412 days (09/15/2010–10/11/2011). Sediment trap cups sampled during sequential intervals of 17 days except the last cup that sampled for 21 days. The second sampling period (T2) continuously operated for 365 days (11/03/2011–11/02/2012) and the sediment trap cups sampled for 15 days intervals except for the last five cups that sampled for 16 days intervals. Forty-seven samples were obtained from mid-September 2010 (9/15/2010) to mid October 2012 (10/17/12). The 24th sampling cup of T1 (October 2011) was lost during the recovery process. The current meter was equipped with oxygen, turbidity and temperature sensors and it acquired measurements every 10 min.

3.2. Processing of sediment trap samples

Refrigerated (4 °C) sediment trap samples were processed in the

laboratory according to the methodology described in Heussner et al. (1990) to produce aliquot sub-samples. Sub-samples were sieved with 0.4 µm-filtered seawater through a 1 mm nylon mesh. All “swimmers” (organisms that swam actively into the trap and died) were removed with forceps from the mesh. Sieved material was poured into a 2000 ml flask and filled up with 0.4 µm-filtered seawater. The flask was placed in a shaking table to generate homogenized aliquots separated with a robotized peristaltic pump. Aliquots were filtered onto pre-weighted 0.45 µm mesh nitro-cellulose white HAWP Millipore filters and onto pre-weighted Whatman GF/F filters both kinds, 47 mm diameter. Total mass was calculated as the dry mass weight of the filtered subsamples multiplied by the fraction of the aliquot. The total mass flux (TMF) expressed as, $\text{mg m}^{-2} \text{d}^{-1}$, was calculated from the total mass weight divided by the trap collecting area (0.5 m^2) and the sampling period in days.

3.3. Geochemical analyses

Total and organic carbon and total nitrogen were measured with a True Spec Carbon Nitrogen analyser LECO. Organic carbon (OC) was measured in samples pre-treated in a 1 M HCl vapour-bath for 24 h. Inorganic carbon was calculated as the difference between total and organic carbon. The inorganic carbon value was multiplied by 8.3331 to determine the calcium carbonate (CaCO_3) concentration. Carbon related analyses were performed with samples filtered onto Whatman GF/F filters. Biogenic opal content was obtained by sequential alkaline extraction following the Mortlock and Froelich (1989) method modified by DeMaster (1981). Biogenic opal analyses were performed on samples filtered onto nitro-cellulose white HAWP Millipore filters. Lithogenic content equals the difference between the total mass and the sum of the main biogenic components: biogenic opal, CaCO_3 and OM content ($2 \times$ the OC content). Total concentrations of each geochemical component was calculated as the concentration of each subsamples multiplied by the fraction of the aliquot.

3.4. Macroscopic components

Fecal pellet (Fig. 3g), *Posidonia oceanica* detritus (Fig. 3e and f) and foraminifera abundance were counted in aliquots using a Wild, Heerbrugg, (Switzerland) stereomicroscope ($10 \times$). Fecal pellets and *P. oceanica* detritus were measured with an eyepiece micrometer ($\pm 10 \mu\text{m}$). Fecal pellet volume was calculated with the formulas for cylindrical, ellipsoidal and spherical bodies, $V = \frac{4}{3}\pi r^3$, $V = \pi r^2 h$ and $V = \frac{4}{3}\pi r_a r_b r_c$ (where V is volume, r is radius and h is height, assuming that r_a and r_b had the same length in the case of ellipsoidal shapes), respectively. The volume of *P. oceanica* detritus was calculated with the formula of cylindrical bodies. Foraminifera tests were counted as single units regardless of their individual size. Pelagic (Fig. 3a and b) and benthic foraminifera (Fig. 3c and d) were differentiated based on the existing taxonomic works on Mediterranean foraminifera (Colom, 1974).

Additionally, images of selected samples were obtained with a Scanning Electron Microscope (SEM) HITACHI S-3500N at 5.0 kV.

3.5. Wind and precipitation

The Spanish Meteorological Agency (AEMET) provided hourly data on precipitation, wind velocity and heading, obtained from the Maó Airport meteorological station ($39^\circ 51' 50.04'' \text{N}$, $004^\circ 13' 26.04'' \text{E}$, 91 m above the sea level) located ~ 17 km from the Menorca canyon's head. For each sampling cup interval we calculated: total precipitation, heading percentages (based on individual observations over the total) and maximum wind velocity values. Additionally, for each sampling interval, hourly wind velocity percentages were grouped from 0 to 60 km h^{-1} into 10 km h^{-1} intervals.

3.6. Wave height

Data on significant wave height events (H_s) were obtained from two oceanographic buoys of the “Puertos del Estado” (Spanish Ports Authority), the Capdepera ($39^\circ 39' 00'' \text{N}$, $003^\circ 29' 2'' \text{E}$) and the Mahón buoys ($39^\circ 25' 04'' \text{N}$, $004^\circ 25' 19''$), located 50 km and 32 km from the canyon's head, respectively.

3.7. Chlorophyll-a concentration and sea surface salinity

Daily superficial chlorophyll a (Chl-a) concentration of the southern coast of Menorca Island and monthly average Chl-a concentration maps of the southern part of the Balearic subbasin and most of the Algerian subbasin were obtained from the satellite database of the Ocean Color Climate Change Initiative project (oceancolor.gsfc.nasa.gov/cms/). Daily satellite-derived Sea Surface Salinity (SSS) maps from the Marine Copernicus Environmental Monitoring Services (<http://marine.copernicus.eu/web/69-interactive-catalogue.php>) were revised in order to identify fronts or eddies in the study area.

3.8. Statistical analyses

Distance-based permutational multivariate analysis of variance (PERMANOVA) (Anderson, 2001) was used to test the null hypothesis of no significant differences between T1 and T2 fluxes. Each term of the analysis was tested using 9999 permutations. Previous to the analysis data were standardized respect to their mean absolute deviation ($MAD = \frac{1}{n} \sum_{j=1}^n [x_{ij} - \bar{x}_i]$ where x_i is the value of the i variable observed in the n colonies) (García Pérez, 2005). The PERMANOVA was performed with the PaST software (Hammer et al., 2001). In order to explore the relationship among the TMF magnitude and the fluxes of its geochemical (CaCO_3 , the lithogenic fraction, OC and biogenic opal) and macroscopic components (fecal pellet, *P. oceanica* detritus and foraminifera) simple linear regression analyses were performed using the lm function (Chambers, 1992) of the R software platform (R Development Core Team, 2014); T1 and T2 data were considered separately.

4. Results

4.1. Total mass flux and geochemical components

The average TMF in T1 was of $1023 \pm 388 \text{ mg m}^{-2} \text{d}^{-1}$ (SD), maximum TMF occurred during early summer (July 2011, $2063 \text{ mg m}^{-2} \text{d}^{-1}$) and smallest during early winter (January 2011, $478 \text{ mg m}^{-2} \text{d}^{-1}$). Two other TMF peaks ($> 1400 \text{ mg m}^{-2} \text{d}^{-1}$) were observed, one during mid autumn 2010, and the other during late summer 2011 (Fig. 2). The average TMF in T2 was $1078 \pm 453 \text{ mg m}^{-2} \text{d}^{-1}$ (SD), the highest TMF occurred in mid autumn 2012 (November 2012, $2304.8 \text{ mg m}^{-2} \text{d}^{-1}$), and the lowest in mid autumn 2011 (November 2011, $191.1 \text{ mg m}^{-2} \text{d}^{-1}$) (Fig. 2). Three other peaks ($> 1400 \text{ mg m}^{-2} \text{d}^{-1}$) were observed (Fig. 2). The first two peaks occurred during early and mid spring (March and April 2012), and the third peak occurred during late summer 2012 (August 2012) (Fig. 2). In T1 and T2, the major geochemical components followed the same pattern as the TMF with the exception of biogenic opal (Fig. 2). The average biogenic opal flux in T1 was of $19 \pm 6.7 \text{ mg m}^{-2} \text{d}^{-1}$ (SD), maximum fluxes were found in mid autumn and late spring (October 2010 and June 2011, 30 and $34 \text{ mg m}^{-2} \text{d}^{-1}$, respectively), lowest fluxes were found in winter (January 2011, $8.9 \text{ mg m}^{-2} \text{d}^{-1}$) (Fig. 2). In T2, the average biogenic opal flux was $21 \pm 11.1 \text{ mg m}^{-2} \text{d}^{-1}$ (SD), maximum fluxes were registered in early summer (June 2012, $40 \text{ mg m}^{-2} \text{d}^{-1}$), and the lowest flux were registered in winter (January 2012, $4.2 \text{ mg m}^{-2} \text{d}^{-1}$) (Fig. 2). Average TMF and geochemical component fluxes for T1 and T2 are depicted in Table 1.

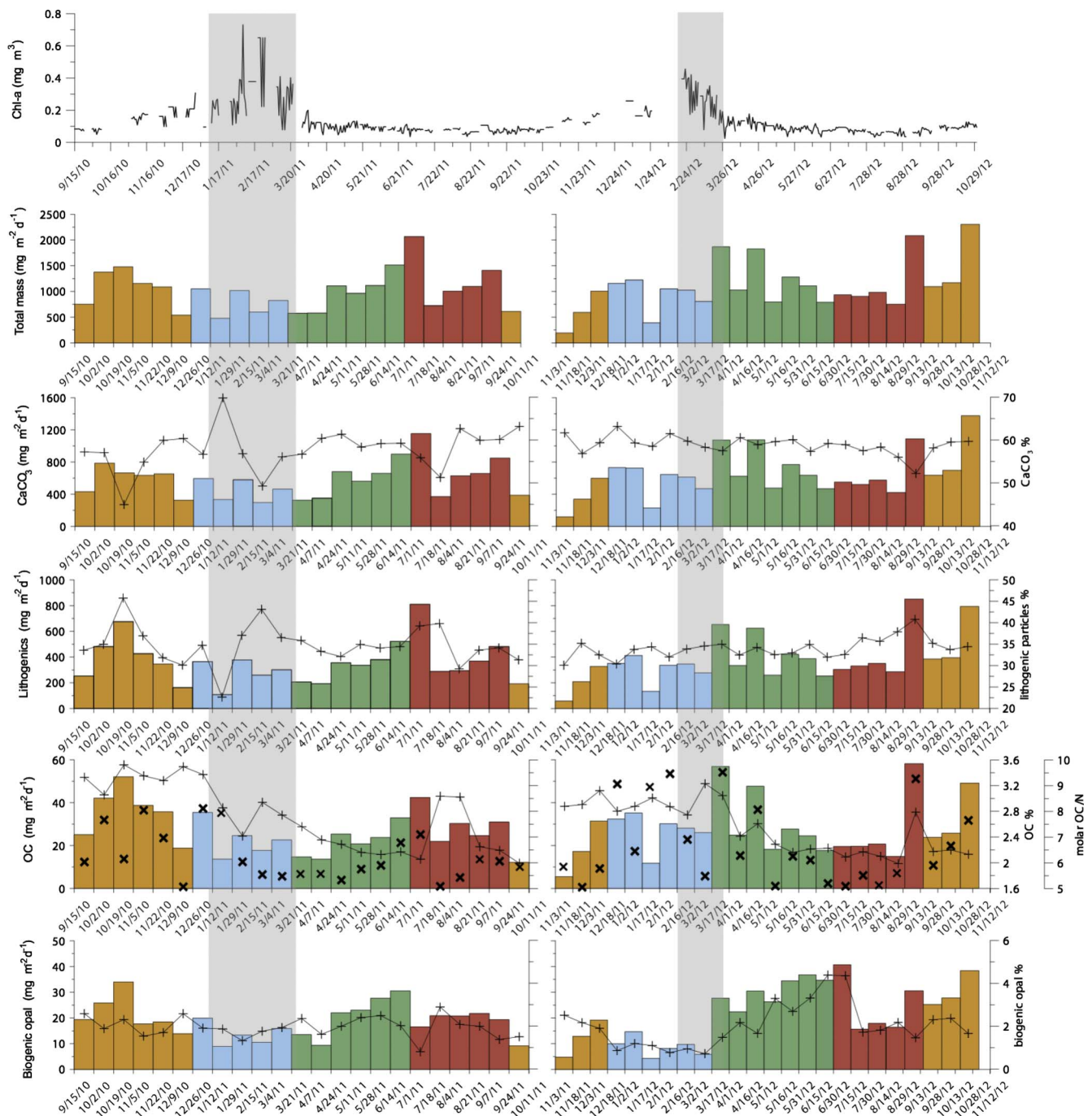


Fig. 2. Time series of daily surface Chl-a concentration, total mass, and the major geochemical constituent fluxes. Gray bands indicate the period with highest surface Chl-a concentration. Connected black crosses represent each constituent percentage and the black crosses represent the OC/N (mol) values. The different bar colours indicate the sampling season (autumn = orange, blue = winter, green = spring, summer = red). (For interpretation of the references to colour in this figure legend, the reader is referred to the web version of this article.)

Fluxes of CaCO_3 and the lithogenic fraction were significantly correlated with TMF ($p < .01$ in both T1 and T2) (linear correlation results in [Supplementary material 1](#)). OC fluxes were also significantly correlated with TMF ($p < .01$ both T1 and T2); however, correlations were weaker during T1 ($R^2 = 0.678$) than during T2 ($R^2 = 0.922$) ([Supplementary material 1](#)). During both T1 and T2, CaCO_3 fluxes were the largest fraction of the TMF contributing 44–70%, the lithogenic fraction was the second most abundant component of the TMF ranging between 22% and 45%. OC contributed between 2% and 3% of the TMF. Biogenic opal fluxes contributed between 0.7% and 4% to the TMF.

No significant differences were found between T1 and T2 when

comparing the magnitude of the TMF and the fluxes of the geochemical components ([Table 1](#)).

4.2. Macroscopic characterization

The average fecal pellet ([Fig. 3 g](#)) flux in T1 was of $10.1 \cdot 10^5 \pm 8.05 \cdot 10^5 \mu\text{m}^3 \text{m}^{-2} \text{d}^{-1}$ (SD), the maximum fecal pellet flux occurred during mid-summer (August 2011, $33.2 \cdot 10^5 \mu\text{m}^3 \text{m}^{-2} \text{d}^{-1}$) and the smallest was found in late winter (March 2011, $0.15 \cdot 10^5 \mu\text{m}^3 \text{m}^{-2} \text{d}^{-1}$). In T2, the average fecal pellet flux was $17.9 \cdot 10^6 \pm 41 \cdot 10^6 \mu\text{m}^3 \text{m}^{-2} \text{d}^{-1}$ (SD); maximum fecal pellet fluxes occurred during mid autumn (October

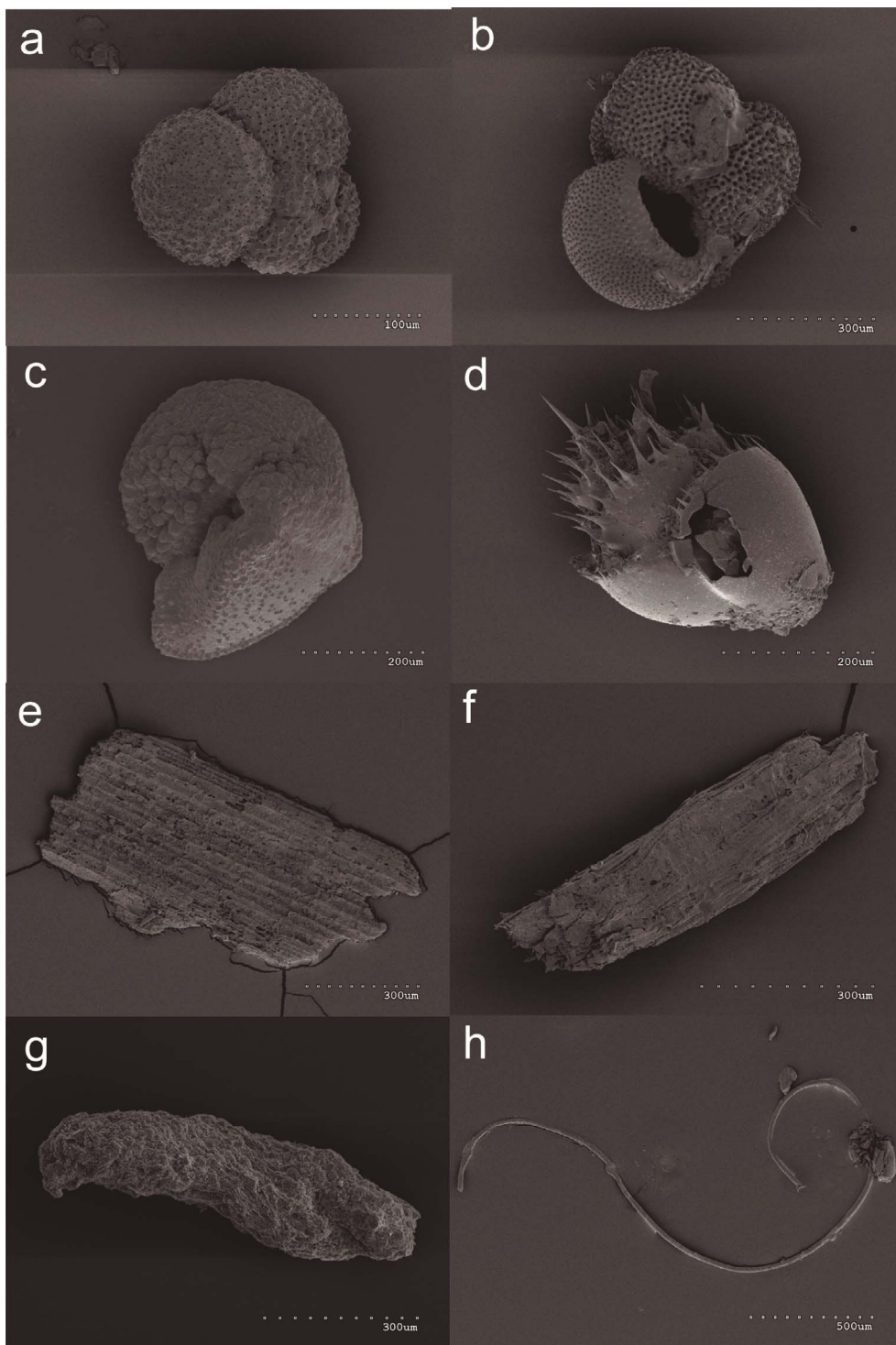


Fig. 3. Scanning electron microscope images of pelagic foraminifera of the genus (a), (b) *Globobulimina*; benthic foraminifera of the genus (c) *Cibicides*, and (d) *Bulimina*, (e), (f) *P. oceanica* detritus, (g) fecal pellet and (h) microplastic fiber.

Table 1
Total mass and geochemical component mean fluxes for T1 and T2 and PERMANOVA analysis. SD = Standard deviation, Litho. = lithogenic, Bio. opal = biogenic opal.

| Fluxes (mg m ⁻² d ⁻¹) | T1 | | T2 | | PERMANOVA | |
|--|-------|-------|------|------|-----------|---------|
| | Mean | SD | Mean | SD | Pseudo-F | p value |
| TMF | 1023 | 388 | 1078 | 453 | 0.179 | .680 |
| CaCO ₃ | 585.6 | 216.6 | 586 | 235 | 0.406 | .535 |
| Litho. | 362 | 166 | 370 | 185 | 0.022 | .887 |
| OC | 26 | 10 | 27 | 13 | 0.018 | .898 |
| Bio. opal | 19 | 6.7 | 21 | 11.1 | 0.385 | .534 |

2012, $162.5 \cdot 10^6 \pm 41 \cdot 10^6 \mu\text{m}^3 \text{m}^{-2} \text{d}^{-1}$), and the lowest flux was registered during late spring (June 2012, $0.5 \cdot 10^6 \mu\text{m}^3 \text{m}^{-2} \text{d}^{-1}$) (Fig. 4). Fecal pellet fluxes registered in T2 were one order of magnitude larger than those collected during T1 (Fig. 4).

In T1, the average flux of *P. oceanica* detritus (Fig. 3e and f) was $10.7 \cdot 10^5 \pm 6.5 \cdot 10^5 \mu\text{m}^3 \text{m}^{-2} \text{d}^{-1}$ (SD), the maximum flux occurred in mid autumn (October 2010, $30 \cdot 10^5 \mu\text{m}^3 \text{m}^{-2} \text{d}^{-1}$), and the lowest was found in early autumn (September 2010, $0.7 \cdot 10^5 \mu\text{m}^3 \text{m}^{-2} \text{d}^{-1}$) (Fig. 4). In T2, the average flux of *P. oceanica* detritus was of $27.6 \cdot 10^5 \pm 26.5 \cdot 10^5 \mu\text{m}^3 \text{m}^{-2} \text{d}^{-1}$, maximum values were registered during winter (December 2011 and February 2012, $102.6 \cdot 10^5$ and 92

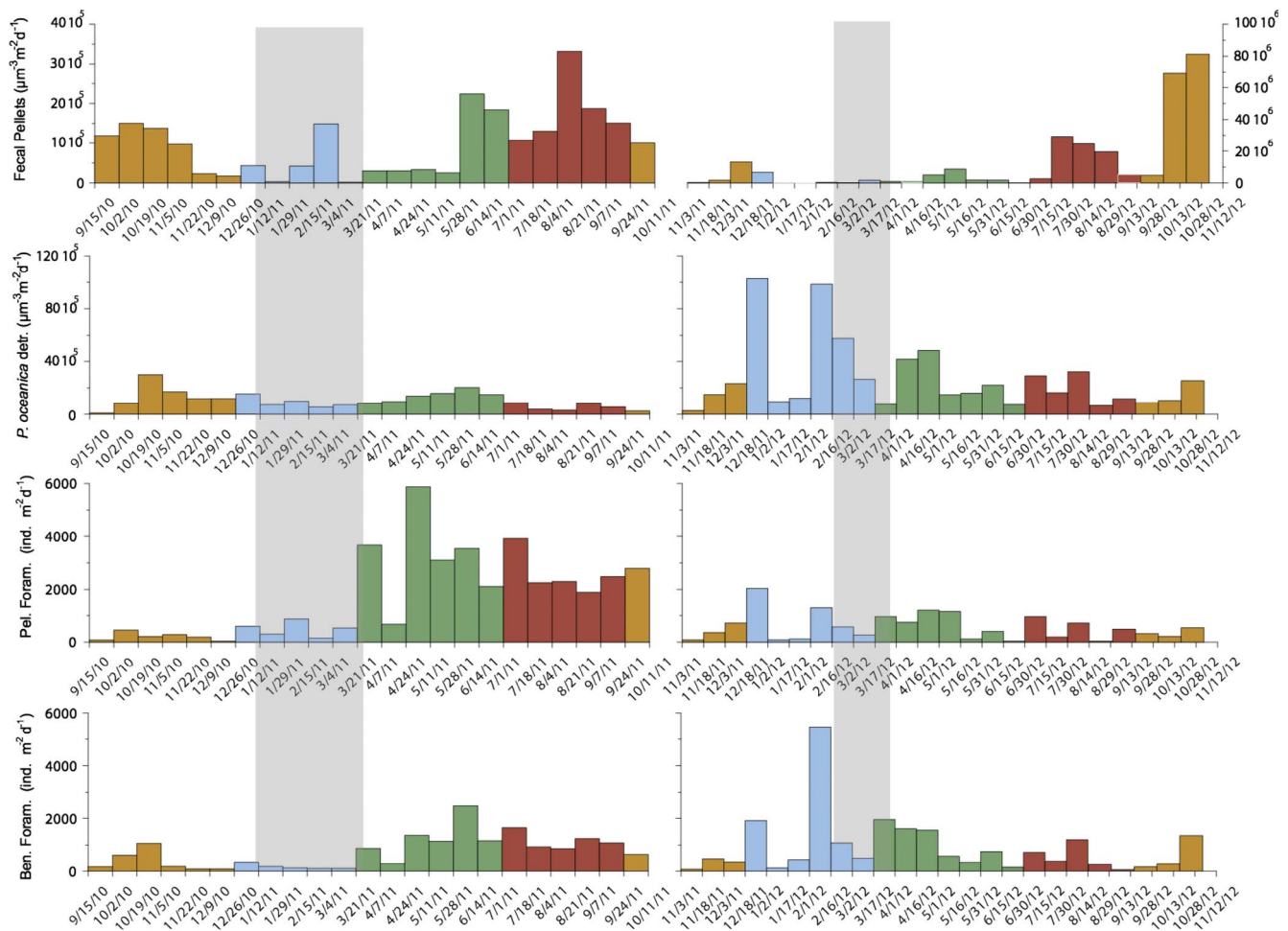


Fig. 4. Time series of fecal pellet, *P. oceanica* detritus and pelagic and benthic foraminifera fluxes. Gray bands indicate the period with highest surface Chl-*a* concentration. detr = detritus, Pel. Foram. = pelagic foraminifera, Ben. Foram. = benthic foraminifera. The different bar colours indicate the sampling season (fall = orange, blue = winter, green = spring, summer = red). (For interpretation of the references to colour in this figure legend, the reader is referred to the web version of this article.)

$10^5 \mu\text{m}^3 \text{m}^{-2} \text{d}^{-1}$, and minimum values in mid autumn (October 2011, $2.6 \cdot 10^5 \mu\text{m}^3 \text{m}^{-2} \text{d}^{-1}$) (Fig. 4).

In T1, average fluxes of pelagic (Fig. 3a and b) and benthic foraminifera (Fig. 3c and d) were $1666 \pm 1602 \text{ ind. m}^{-2} \text{d}^{-1}$ (SD) and $725 \pm 620 \text{ ind. m}^{-2} \text{d}^{-1}$ (SD), respectively. Maximum pelagic and benthic foraminifera fluxes occurred in spring (April 2011, $5900 \text{ ind. m}^{-2} \text{d}^{-1}$ for pelagic foraminifera and May 2011, $2500 \text{ ind. m}^{-2} \text{d}^{-1}$ for benthic foraminifera), while the lowest fluxes were found in late autumn (early December 2010, $75 \text{ ind. m}^{-2} \text{d}^{-1}$ for pelagic and $180 \text{ ind. m}^{-2} \text{d}^{-1}$ for benthic foraminifera) (Fig. 4). In T2, average pelagic and benthic foraminifera fluxes were $613 \pm 657 \text{ ind. m}^{-2} \text{d}^{-1}$ (SD) and $968 \pm 1160 \text{ ind. m}^{-2} \text{d}^{-1}$ (SD), respectively (Fig. 4). Maximum pelagic and benthic foraminifera fluxes were registered during winter (December 2011, $2040 \text{ ind. m}^{-2} \text{d}^{-1}$ for pelagic foraminifera and February 2012, $1920 \text{ ind. m}^{-2} \text{d}^{-1}$ for benthic foraminifera), while lowest fluxes were found during summer (August 2012, $54 \text{ ind. m}^{-2} \text{d}^{-1}$ for pelagic and $36 \text{ ind. m}^{-2} \text{d}^{-1}$ for benthic foraminifera) (Fig. 4).

Average fecal pellets and *P. oceanica* detritus volumes were significantly larger in T2 (Table 2). Conversely, the average fluxes of pelagic foraminifera were significantly larger during T1 (Table 2). No significant differences were found among benthic foraminifera fluxes and sampling periods (Table 2).

None of the macroscopic components fluxes were significantly correlated with TMF (linear correlation results in Supplementary material 2). Microplastic fibers were found in all sampling cups for both T1 and T2 (Fig. 3 h). However, due to their irregular shape and small dimensions they were not quantified.

Table 2

Mean fluxes of the macroscopic components for T1 and T2 and PERMANOVA analysis. SD = Standard deviation, detr. = detritus.

| Fluxes $\mu\text{m}^3 \text{m}^{-2} \text{d}^{-1}$ / $\text{ind. m}^{-2} \text{d}^{-1}$ * | T1 | | T2 | | PERMANOVA | |
|---|-------------------|------------------|-------------------|-------------------|-----------|---------|
| | Mean | SD | Mean | SD | Pseudo-F | p value |
| Fecal pellets | $10.1 \cdot 10^5$ | $8 \cdot 10^5$ | $17.9 \cdot 10^6$ | $41 \cdot 10^6$ | 3.54 | .011 |
| <i>P. oceanica</i> detr. | $10.7 \cdot 10^5$ | $6.5 \cdot 10^5$ | $27.6 \cdot 10^5$ | $26.5 \cdot 10^5$ | 8.52 | .001 |
| Pel. Foram.* | 1666 | 1602 | 613 | 657 | 5.95 | .016 |
| Bent Foram.* | 725 | 620 | 968.5 | 1160 | 6.75 | .010 |

4.3. Environmental factors

4.3.1. Currents, turbidity and oxygen content

During both sampling periods water current mainly followed a north–south direction (Fig. 5). Average current velocity during T1 and T2 were 3.5 cm s^{-1} and 4.4 cm s^{-1} , respectively. During both sampling periods, current velocity rarely exceeded 20 cm s^{-1} . During most of T1, turbidity values were low ($< 0.27 \text{ NTU}$); however, after mid spring values increased and remained above 0.28 NTU for most of the remaining sampling period. Simultaneously to this turbidity increment a substantial reduction in dissolved oxygen was observed. During most of T2 turbidity remained very low except for two punctual increments, one in mid-summer (July 2012) and a second in early winter (November 2012) (Fig. 5).

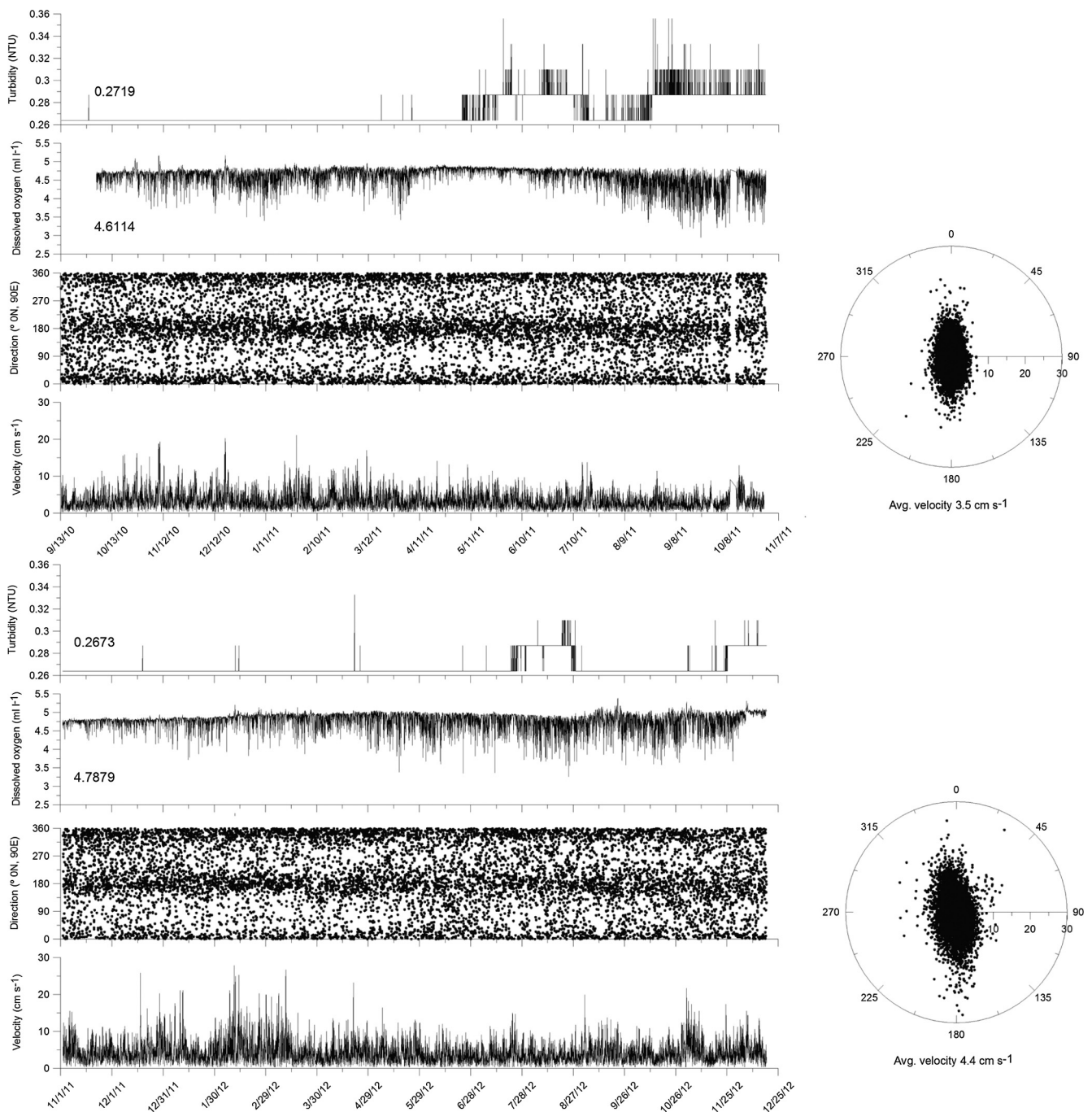


Fig. 5. Times series plots of turbidity, dissolved oxygen and current direction and velocity during T1 and T2 sampling intervals. The numbers within turbidity and dissolved oxygen charts indicate average values.

4.3.2. Wind and precipitation

During T1, the highest precipitation rates were registered during mid-September 2010 to mid-November 2010 ranging from 818 ml/m³ to 2430 ml/m³. During T2, the highest precipitation rates were registered during November 2011 and 2012 and February 2012 with values around 912 ml/m³, 3112 ml/m³ and 1090 ml/m³, respectively. Northerly winds were dominant during both sampling periods representing 47.9% and 45.9% of total hourly wind registers for T1 and T2, respectively. Windiest episodes were registered during January and February for both T1 and T2. During this period the percentage of the hourly winds exceeding 30 km/h ranged between 10% and 14% in T1 and between 7% and 46% in T2.

4.3.3. Wave height

Waves between 1 and 2 m high were the most frequent size class representing 88% and 72% of registered waves in the Capdepera and Mahón buoys, respectively. Significant wave height events (3.5–5 m height) mostly occurred during winter, were generally associated to high wind speeds (> 40 km h⁻¹) (Table 3) and mainly presented a N and NNE orientation. Few of the significant wave height events occurred during periods of heavy precipitations (Table 3). Only two out of 36 significant wave height events registered during this study coincided with TMF peaks (Table 3).

Table 3

Significant wave height events during both sampling intervals. Max. WH = maximum wave height. Gray rows indicate those events that coincided with total mass flux peaks. Max. WS = maximum wind speed.

| Date | Max. WH (m) | | Max. WS (km/h) | Precipitation (ml/m ³) |
|----------|-------------|-------|----------------|------------------------------------|
| | Capdepera | Mahón | | |
| 10/18/10 | 4.07 | - | 44 | 0 |
| 10/25/10 | 4.25 | - | 50 | 41 |
| 11/02/10 | 4.08 | - | 46 | 46 |
| 12/15/10 | 5 | 5.38 | 53 | 0 |
| 12/24/10 | - | 5.24 | 29 | 48 |
| 12/26/10 | 3.8 | 5.36 | 53 | 18 |
| 01/12/11 | - | 5.03 | 37 | 0 |
| 01/21/11 | 3.5 | 5.90 | 36 | 0 |
| 02/02/11 | 3.78 | 4.81 | 51 | 0 |
| 02/27/11 | - | 4.75 | 48 | 47 |
| 03/01/11 | 4.02 | - | 47 | 194 |
| 03/08/11 | 3.98 | - | 36 | 0 |
| 03/18/11 | - | 3.97 | 25 | 0 |
| 03/20/11 | - | 3.60 | 40 | 0 |
| 05/15/11 | - | 3.83 | 65 | 0 |
| 06/01/11 | - | 4.52 | 54 | 15 |
| 08/10/11 | 4.57 | 4.97 | 57 | 0 |
| 09/20/11 | - | 4.13 | 36 | 10 |
| 12/16/11 | - | 5 | 43 | 119 |
| 12/18/11 | - | 4.25 | 28 | 0 |
| 12/19/11 | 4.13 | - | 28 | 0 |
| 12/21/11 | - | 4.21 | 38 | 284 |
| 12/24/11 | 4.17 | 5.50 | 51 | 0 |
| 12/30/11 | 4.23 | 5.57 | 41 | 0 |
| 01/04/12 | - | 4.25 | 25 | 0 |
| 01/06/12 | 4.69 | 5.39 | 60 | 0 |
| 01/07/12 | - | 5.23 | 41 | 0 |
| 01/09/12 | - | 4.02 | 37 | 0 |
| 24/01/12 | - | 4.12 | 32 | 0 |
| 30/01/12 | - | 5.18 | 54 | 2 |
| 02/03/12 | 4.88 | 6.37 | 58 | 62 |
| 02/04/12 | - | 6.18 | 46 | 1 |
| 02/07/12 | 4.86 | 6.05 | 49 | 0 |
| 03/05/12 | 3.57 | - | 61 | 2 |
| 04/17/12 | - | 5.38 | 49 | 0 |
| 09/14/12 | 3.74 | - | 55 | 0 |

4.3.4. Chlorophyll-*a* concentration and sea surface salinity

During T1 and T2, Chl-*a* superficial concentration progressively increased from mid-October to early February when it reached its maximum values of $\sim 0.7 \text{ mg m}^{-3}$ and $\sim 0.4 \text{ mg m}^{-3}$ for T1 and T2, respectively (Fig. 2). In both T1 and T2, lowest Chl-*a* concentrations ranging between $\sim 0.2 \text{ mg m}^{-3}$ and $\sim 0.1 \text{ mg m}^{-3}$, were registered from early April to early October (Figs. 2, 6 and 7).

Sea surface salinity maps revealed that from September 2010 until February 2011 resident AW (salinities > 37.5) occupied the southern slope of Balearic archipelago (Fig. 8). However, from March 2011 until August 2011 fresher recent AW (salinities < 37.5) progressively moved northward from the Algerian sub-basin and reached the southern slope of the archipelago (Fig. 8). Moreover, an eddy was present in the southern slope of Menorca from June to August 2011 remaining in this area for approximately 75 days (Fig. 8).

During the T2, sea surface salinity was comparatively stable and no major intrusions of fresher recent AW were observed in the southern slope of the archipelago (Fig. 9).

5. Discussion

5.1. Total mass flux in the Menorca canyon head in the Mediterranean context

TMF in the Menorca canyon were smaller than those registered in other western Mediterranean submarine canyon heads (Table 4). TMF in the present study were also smaller than TMF in other Mediterranean canyon axes and adjacent slopes regardless of depth, indicating that this insular canyon is among those with the most sediment-starved conditions in the Western Mediterranean (Table 4). The TMF range in the Menorca canyon was comparable to those observed in the deep continental margin of the Alboran Sea (Sanchez-Vidal et al., 2005) and the open slope of the southern Adriatic Sea (Miserocchi et al., 1999).

However, TMF in the Menorca canyon did exceed those collected in the southern and northern Balearic slopes (Table 4; Danovaro et al., 1999). Based on this comparison, the present results corroborate previous observations that indicated that the Menorca canyon acts as a sediment conduit from the continental shelf to deeper environments (Acosta et al., 2002), also in agreement with the general pattern observed in most Mediterranean canyons (e.g. Monaco et al., 1990; Martín et al., 2006).

In Mediterranean submarine canyons related to fluvial systems and

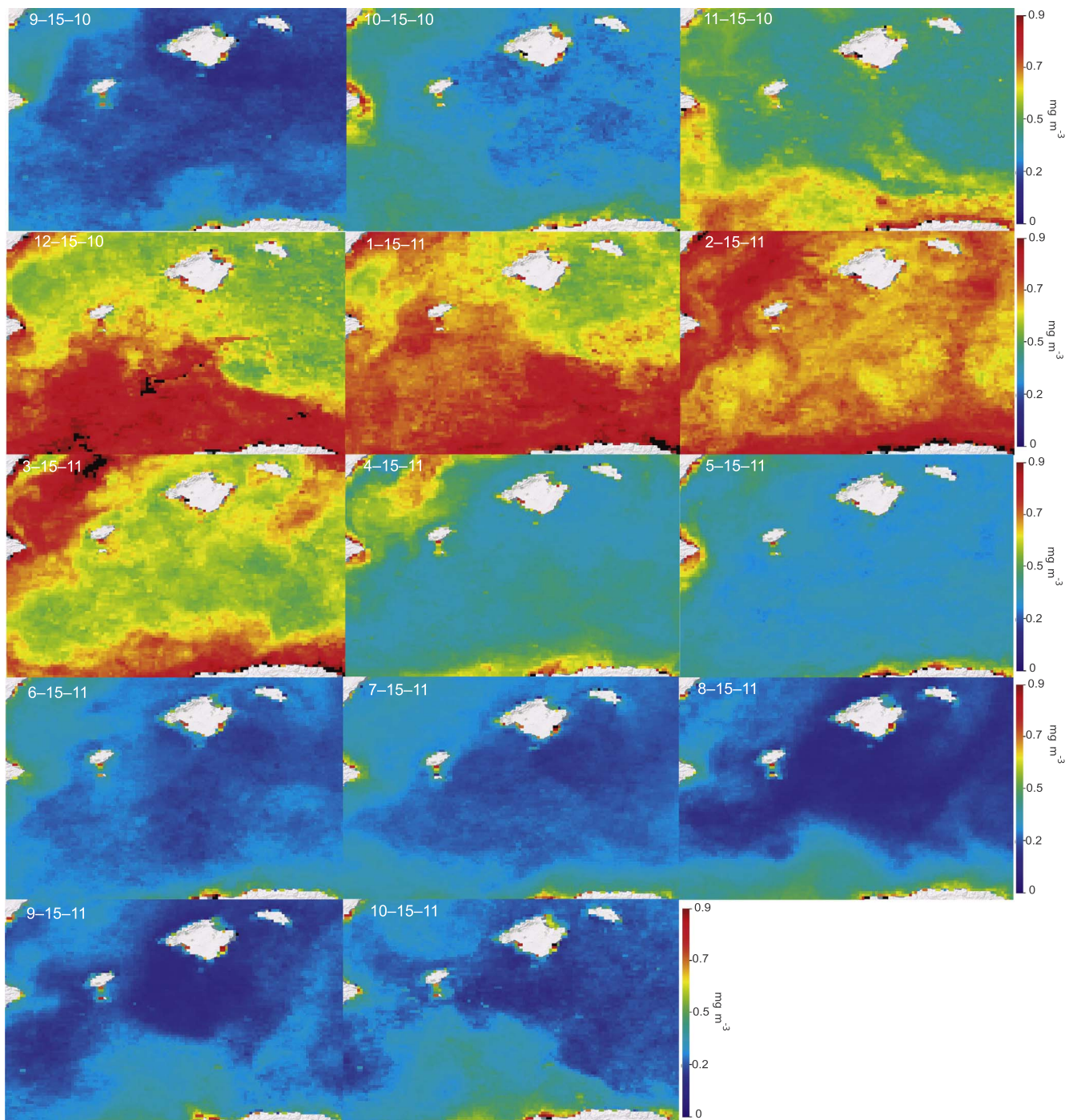


Fig. 6. Horizontal distribution of monthly averaged Chl-a surface concentration during T1.

affected by intense across slope current events (Table 4) the largest annual TMF fluxes mainly occur during winter (e.g. Martín et al., 2006; Lopez-Fernandez et al., 2013b), which can account for more than 40% of the yearly TMF (e.g. Durrieu de Madron et al., 1999; Pasqual et al., 2010). They can be triggered by intense short term meteorological events, such as winter precipitation that causes river flooding (Palanques et al., 2005; Zúñiga et al., 2009; Lopez-Fernandez et al., 2013b), wave height events associated with storms (Durrieu de Madron et al., 1999; Martín et al., 2006; López-Fernandez et al., 2013b), and North winds that may induce cascading processes (Pasqual et al., 2010). Conversely, in the Menorca canyon winter TMF were the smallest accounting for 17% and 19% of the bulk TMF for T1 and T2, respectively. Moreover, during winter more than twenty wave height events were

registered in the study area (Table 3) and none of them was associated with a TMF peak. Episodic river systems can also trigger hyperpycnal flows delivering large amounts of sediment over brief periods of time (Katz et al., 2015). Approximately thirty small episodic river systems arrive to Menorca's southern shore. In spite of this, TMF remained low and no increments in turbidity were observed during winter months when very high precipitation rates occurred during both T1 and T2. Thus, the contribution of episodic river systems to the TMF appears to be negligible in this area. Therefore, we conclude that the influence of meteorological events on TMF in the Menorca canyon head is not as significant as in most Western Mediterranean canyons, and we suggest that this trend is accentuated by the absence of permanent river systems that provide terrestrial material to Menorca's southern margin.

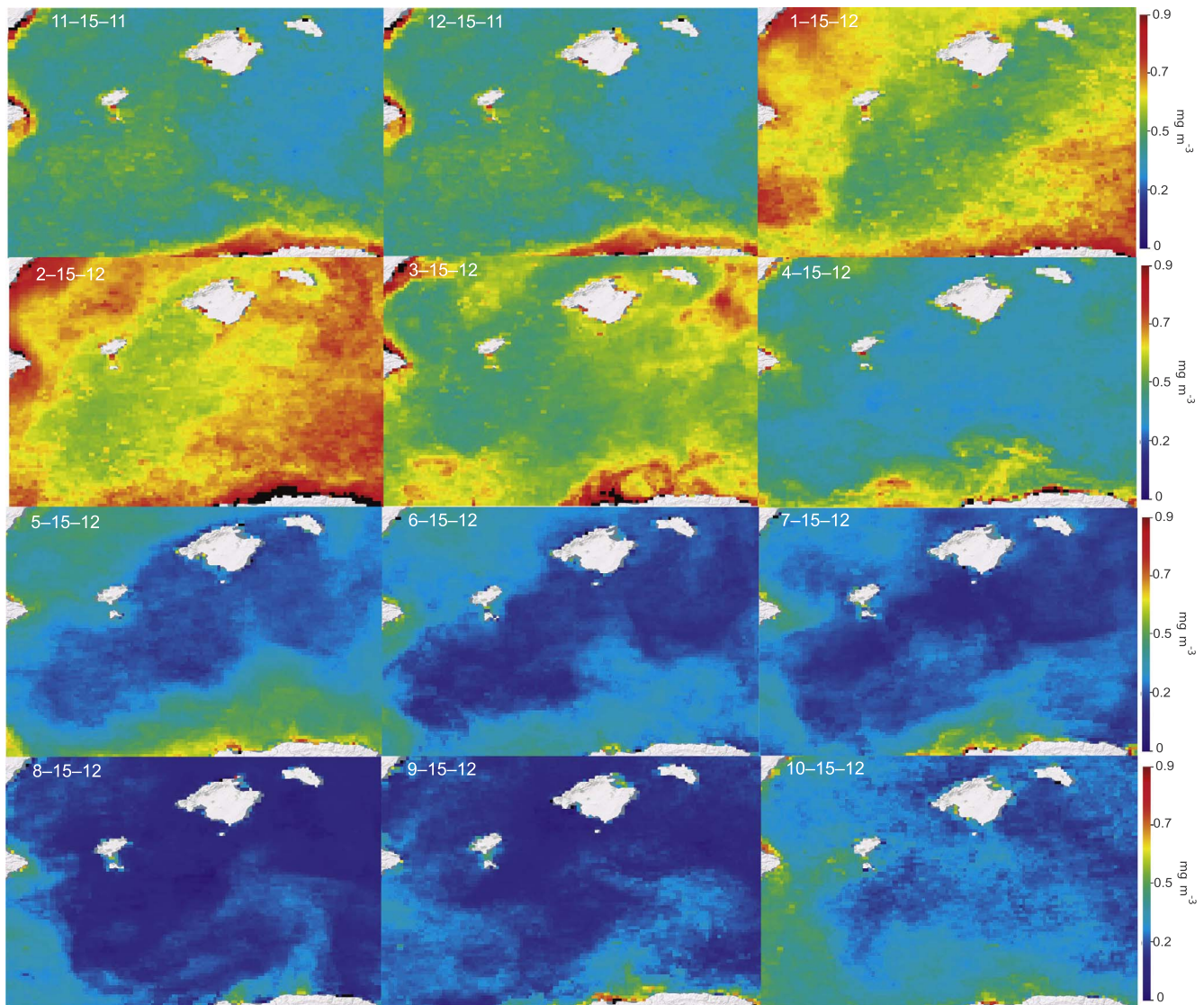


Fig. 7. Horizontal distribution of monthly averaged Chl-a surface concentration during T2.

A relationship between the width of the continental shelf and particle fluxes has been observed in river-dominated continental shelves with high sediment supplies and sediment deposits (Walsh and Nittrouer, 2009). The width of the continental shelf modulates the amount of sediment reaching the shelf edge and upper slope (Walsh and Nittrouer, 2009). In narrow continental shelves sediment can be rapidly mobilized to deeper areas under the influence of storms and river flooding (Walsh and Nittrouer, 2003; Puig et al., 2004). However, in our results the lack of a clear relationship between storms, precipitation and other meteorological events and sediment fluxes suggests that in sediment starved margins such as the one considered in this study it seems unlikely that the width of the continental shelf (between 3 and 6 km) may play a key role modulating downward particle fluxes.

5.2. Total mass flux peak driving mechanisms

In the Menorca canyon only few particle flux peaks coincided with meteorological or hydrodynamic events, which could resuspend and transport particulate material. The peaks observed during mid autumn 2010 (October 2010) and mid spring 2012 (April 2012) (Fig. 2) coincided with significant wave height events ($H_s = > 3.5$ m) (Table 3), which are potential inner shelf bottom sediment resuspension drivers (Guillén et al., 2006; Ulses et al., 2008). These peaks were characterized

by a slight increment in turbidity and the lithogenic fraction (Figs. 2 and 5), providing further support to this hypothesis, also in agreement with previous observations in other submarine canyons in the western Mediterranean (Martín et al., 2006).

During July 2011 a peak in TMF occurred (Fig. 2). Coinciding with this peak an anticyclonic eddy developed over the southern slope of Menorca (Fig. 8). In the Mediterranean Sea eddies have been reported to extend to great depth (> 2000 m) and occasionally reaching the sea floor (Durrieu de Madron et al., 2017). In these cases, eddies alter the direction and velocity of bottom currents causing sediment resuspension (O'Brien et al., 2013; Amores et al., 2013, 2014). Although it is unclear whether the effects of this eddy reached the mooring site (it was not clearly detected in the current meter), this TMF peak was associated with a slight increment in turbidity (Fig. 5) and the lithogenic fraction, suggesting that it was caused by sediment resuspension. The positive effect of this water bodies on the increase in TMF, turbidity and the lithogenic fraction has also been observed in other sediment starved environments such as the northern Balearic margin (Amores et al., 2013; Pasqual et al., 2014).

TMF peaks occurring during late summer 2011 (September 2011), and late summer and mid autumn 2012 (Fig. 2, August and October 2012) were associated with slight increments in the lithogenic fraction and turbidity, indicating a possible association with resuspension

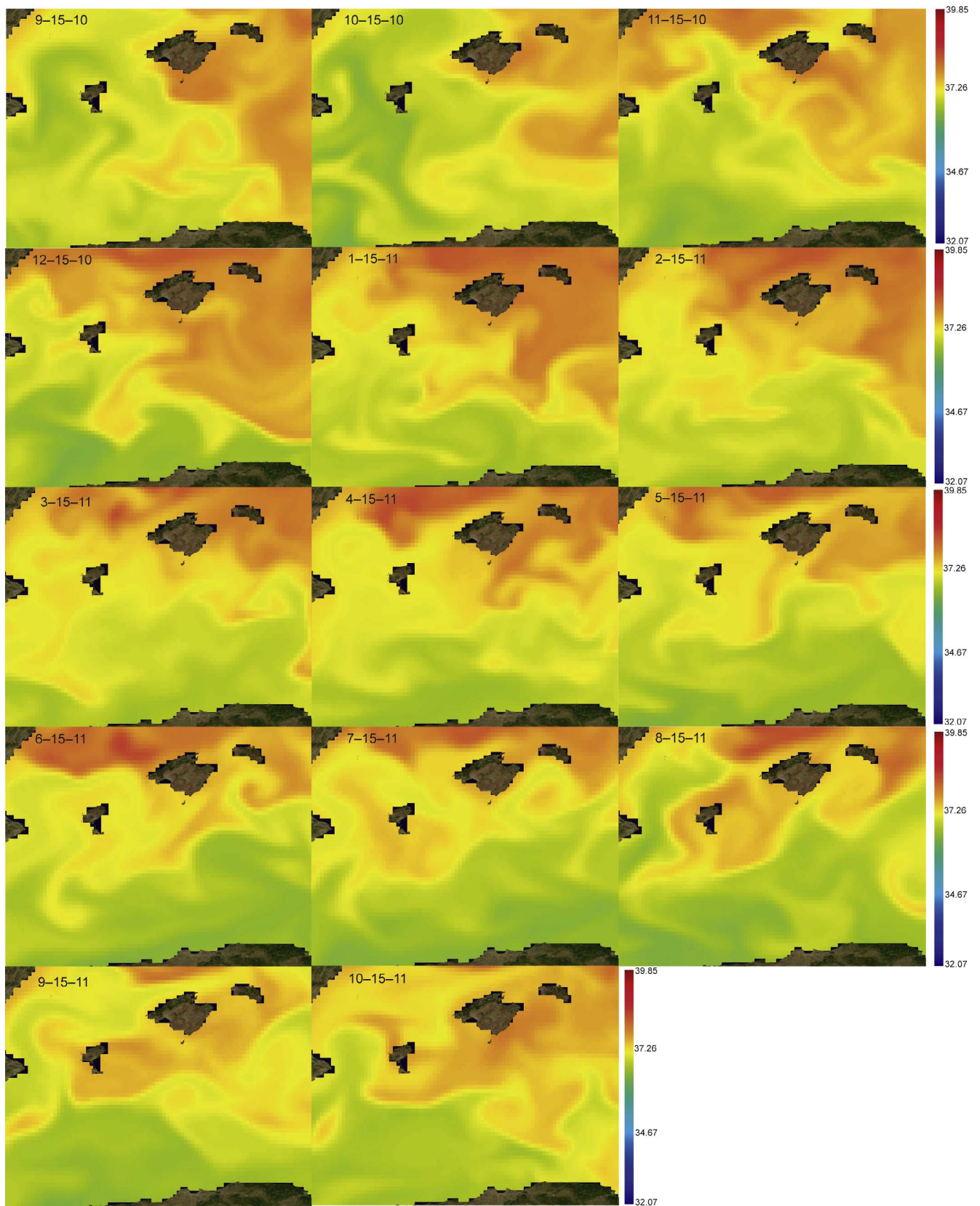


Fig. 8. Sea surface salinity maps of the 15th day of every month during T1. Salinity values were extracted at 1.47 m depth.

processes too (Martín et al., 2006). However, the mechanisms that could have triggered such processes remain unclear since no concomitant strong bottom currents, meteorological or hydrodynamic events were observed (Figs. 5, 8, 9 and Table 3).

In other areas of the Balearic Archipelago, internal waves have been associated with high TMF (Pasqual et al., 2015). The interaction of internal waves with the seafloor may cause current acceleration, turbulent flows, and sediment resuspension (Pasqual et al., 2015; Ribó

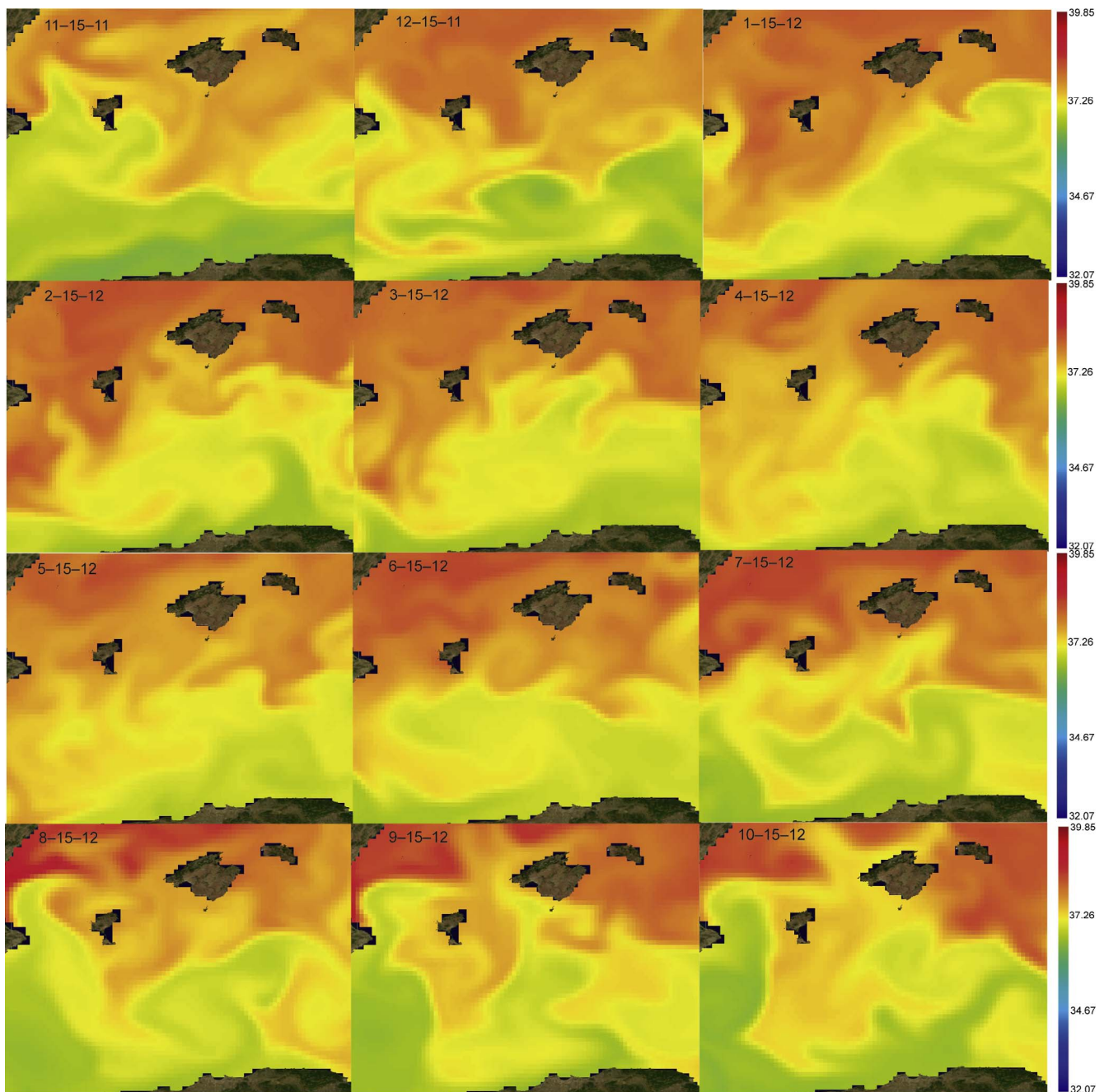


Fig. 9. Sea surface salinity maps of the 15th day of every month during T2. Salinity values were extracted at 1.47 m depth.

et al., 2016). However, it is unlikely that the aforementioned peaks were triggered by internal waves as no increments in current velocity were observed (Pasqual et al., 2015). The influence of internal waves on TMF would be more evident on environments where a substantial source of fine sediment is readily available for resuspension (Quaresma et al., 2007), which it seems not to be the case in the present study. Bottom trawling has also been related to increments in TMF without any evident relationship with natural forcing mechanisms (Martín et al., 2006; Palanques et al., 2006). Trawling can cause abrupt sediment resuspension enhancing turbidity and particle fluxes (Martín et al., 2006; Palanques et al., 2006). However, it is unlikely that the observed particle flux peaks derive from this fishing practice given that, in the study area, trawling is mostly conducted below 500 m (Moranta et al., 2014; Grinyó, 2016).

In other areas of the Mediterranean, spring and summer TMF peaks have been associated with primary production blooms (Sanchez-Vidal

et al., 2005; Stavrakakis et al., 2013) characterized by material with relatively high organic carbon and opal concentrations (Sanchez-Vidal et al., 2005) derived from exports of the euphotic zone (Rigual-Hernández et al., 2013). In our study, only the peak in March 2012 coincided with the winter-spring bloom and showed high organic carbon content; although, low opal percentages (Fig. 2), which would suggest that non-siliceous phytoplankton dominated the bloom. However, the high OC/N ratio (9.5 M OC/N) registered during this peak (Fig. 2) indicates that the collected organic matter was degraded, and most likely derived from resuspension processes (Martín et al., 2011). This would imply that the input of resuspended material during this spring peak to the TMF was greater than the one derived from pelagic production, in contrast with the spring trend observed in other Mediterranean canyons and open sea environments (e.g. Sanchez-Vidal et al., 2005; Stavrakakis et al., 2013).

Table 4
Register of TMF and geochemical constituents in Mediterranean submarine canyons and slopes. Med. = Mediterranean, S Adr = South Adriatic, Lig. = Ligurian, GL = Gulf of Lions, Cat. Mar. = Balearic Archipelago, Alb. = Alborán Sea, For. Mech. = forcing mechanism, am = annual mean, twf = time weighted flux, CCC = Cap de Creus canyon, LDC = Lacaze-Duthiers canyon, PP = primary production, R = resuspension, NADW = North Adriatic dense Sea Water, RF = river flood, S = storm, SD = saharan dust, HS = hydrodynamic setting, ~ = approximate values.

| Med. area | Sub-area | Depth (m) | Duration (days) | | | TMF (mg m ⁻² d ⁻¹) | | | Maximum | | | Forc. Mech | Reference |
|-----------|--------------------|-----------|-----------------|---------------|------------|---|-------|------------------|---------|----------------------|------|------------|--------------------------------|
| | | | Trap | Current meter | Sea bottom | Mean | Max | Max. season | Lit.-% | CaCO ₃ -% | OC-% | | |
| Crete | Samaría Canyon | 1246 | 1231 | - | 1246 | 0.332 | ~1.2 | March | - | - | - | PP | Malinverno et al. (2009) |
| Crete | Samaría Canyon | 1316 | 350 | - | 1316 | 0.056 | ~0.1 | September | - | - | - | PP | Malinverno et al. (2009) |
| Crete | Samaría Canyon | 1982 | 1967 | - | 1982 | 0.077 | 0.225 | July | - | - | - | PP | Malinverno et al. (2009) |
| Crete | Samaría Canyon | 3568 | 3553 | - | 3568 | 0.060 | 0.11 | March | - | - | - | PP | Malinverno et al. (2009) |
| Crete | N Cretan Margin | 1150 | 1515 | 1135 | 1150 | 0.209 | 0.459 | March | 68.3 | 52.7 | 3.57 | R/PP | Stavrakakis et al. (2000) |
| S Adr. | Bari Slope | 642 | 607 | 570 | 642 | 1.7 am | 6.8 | March–April–May | - | - | ~2 | NADW | Turchetto et al. (2007) |
| S Adr. | N Bari Canyon | 600 | 565 | 570 | 600 | 3.1 | 15.6 | March–April–May | - | - | ~2 | NADW | Turchetto et al. (2007) |
| S Adr. | S Bari Canyon | 595 | 560 | 570 | 595 | 8.1 | 24.6 | March–April–May | - | - | ~1.4 | NADW | Turchetto et al. (2007) |
| Lig. Sea | Var Canyon | 1280 | 1245 | 1245 | 1280 | - | 120 | December | - | - | 2 | RF | Khripounoff et al. (2012) |
| Lig. Sea | Var Canyon | 1575 | 1555 | 1545 | 1575 | - | 218 | February | - | - | 1.5 | RF | Khripounoff et al. (2012) |
| GL | CCC | 302 | 297 | 297 | 302 | 7.5 | ~30 | Spring | 64.8 | 29.4 | 1.8 | S-DSWC | Bonnin et al. (2008) |
| GL | LCD | 309 | 304 | 304 | 309 | 11.7 | ~110 | Fall | 66.1 | 31.0 | 1.9 | S-DSWC | Bonnin et al. (2008) |
| GL | Aude Canyon | 309 | 304 | 304 | 309 | 7.8 | ~25 | Fall | 65.3 | 31.4 | 1.3 | S-DSWC | Bonnin et al. (2008) |
| GL | Hérault Canyon | 302 | 297 | 297 | 302 | 9.6 | ~75 | Fall | 64.6 | 30.4 | 1.6 | S-DSWC | Bonnin et al. (2008) |
| GL | Petit Rhône Canyon | 302 | 297 | 297 | 302 | 8.6 | ~30 | Fall | 63.8 | 33.1 | 1.9 | S-DSWC | Bonnin et al. (2008) |
| GL | Planiere Canyon | 307 | 84 | 302 | 307 | 3.1 | 3.1 | Fall | 45.1 | 35.1 | 2.5 | S-DSWC | Bonnin et al. (2008) |
| GL | LDC | 645 | 600 | 620 | 645 | 6.02 | 20 | February | 68 | 30 | 7 | S | Courp and Monaco (1990) |
| GL | LDC | 300 | 295 | 295 | 300 | 6.7 | 18.1 | November | 71.6 | 36.6 | 4.1 | DSWC | Pasqual et al. (2010) |
| GL | LDC | 1000 | 995 | 970 | 1000 | 6.7 | 11.2 | January | 68.6 | 42.9 | 5.5 | DSWC | Pasqual et al. (2010) |
| GL | LDC | 1500 | 1495 | 1470 | 1500 | 1.4 | 11.9 | March | 65.8 | 34.9 | 5.4 | DSWC | Pasqual et al. (2010) |
| GL | CCC | 300 | 295 | 270 | 300 | 7.0 | 20 | October | 67.6 | 29 | 3.2 | DSWC | Pasqual et al. (2010) |
| GL | CCC | 1000 | 995 | 970 | 1000 | 11.7 | 90.1 | January | 73.1 | 29.9 | 3.4 | DSWC | Pasqual et al. (2010) |
| GL | CCC | 1500 | 1495 | 1470 | 1500 | 1.3 | 6.3 | January | 68.6 | 36.3 | 9.5 | DSWC | Pasqual et al. (2010) |
| Cat. Mar. | Blanes Canyon | 300 | 275 | 275 | 300 | 12.06 | 82.67 | December | 78.27 | 43 | 7.68 | S-RF | Lopez-Fernandez et al. (2013b) |
| Cat. Mar. | Blanes Canyon | 900 | 875 | 875 | 900 | 14.75 | 35.29 | December | 75.63 | 30.1 | 4.44 | S-RF | Lopez-Fernandez et al. (2013b) |
| Cat. Mar. | Slope | 900 | 875 | 875 | 900 | 3.43 | 7.81 | April | 74.01 | 26.2 | 10.3 | SD | Lopez-Fernandez et al. (2013b) |
| Cat. Mar. | Blanes Canyon | 600 | 570 | 568 | 600 | 14 twf | 40.78 | December | - | 24 | 5.5 | RF | Zúñiga et al. (2009) |
| Cat. Mar. | Palamós Canyon | 470 | 448 | ~446 | 470 | 28.75 | 94 | November | 77 | 33 | 3.5 | S | Martín et al. (2006) |
| Cat. Mar. | Foix Canyon | 600 | 570 | - | 600 | 3.8 am | 19 | July | - | 27.5 | 2 | S-RF | Puig and Palanques (1998) |
| Cat. Mar. | Foix Canyon | 1180 | 1150 | - | 1180 | 12 am | 7.5 | October | - | 28 | ~2.5 | S-RF | Puig and Palanques (1998) |
| Cat. Mar. | Slope | 980 | 950 | - | 980 | 0.8 am | 1.8 | April | - | 30 | 5.9 | S-RF | Puig and Palanques (1998) |
| Bal. Arc. | Menorca Canyon T1 | 430 | 400 | 405 | 430 | 1 | 2.06 | July | 45.7 | 70 | 3.5 | R-HS | Present study |
| Bal. Arc. | Menorca Canyon T2 | 430 | 400 | 405 | 430 | 1.09 | 2.30 | October | 40.7 | 63 | 3.2 | R-HS | Present study |
| Bal. Arc. | N slope Mallorca | 900 | 870 | 870 | 900 | 0.31 | 0.61 | March | 65.2 | 43 | 5.8 | S-RF | Pasqual et al. (2015) |
| Bal. Arc. | S slope Mallorca | 900 | 870 | 870 | 900 | 0.16 | 0.337 | February | 66.4 | 47.3 | 7.1 | PP | Pasqual et al. (2015) |
| Alb. | Guadaro Canyon | 592 | 567 | 567 | 592 | 6.1 | 27.4 | May | ~80 | ~14 | ~2.3 | RF | Palanques et al. (2005) |
| Alb. | Channel | 717 | 692 | 692 | 717 | 1.87 | 5.7 | December–January | ~82 | ~15 | > 5 | RF | Palanques et al. (2005) |
| Alb. | Oppen Slope | 720 | 695 | 695 | 720 | 3.03 | 6 | December | 82 | ~15 | 3 | RF | Palanques et al. (2005) |

5.3. Geochemical components

During T1 and T2, CaCO₃ represented the most abundant fraction (58 ± 4% and 59 ± 2% (SD) respectively). This contrasts with the general trend observed in other Mediterranean canyons, slopes and open sea environments, where lithogenic material constitutes more than 50% of all collected material (Table 4, Fabrés et al., 2002; Stavrakakis et al., 2013). Conversely, the lithogenic fraction in the Menorca canyon barely represents 35% of all collected material. This high CaCO₃ content likely derive from the dense calcareous algae assemblages located in the adjacent continental shelf (maërl and rhodolites) that are characterized by high carbonate production (Canals and Ballesteros, 1997), and also because most inland sources are characterized by carbonated rocks (Obrador et al., 1992). In this sense, surface sediments in the adjacent shelf and slope present similar CaCO₃ contents (Alonso et al., 1988) to those found in T1 and T2. This similitude suggests that most CaCO₃ collected during both sampling periods derived from resuspended matter in adjacent environments that was transported along the canyon; agreeing with previous hypotheses on CaCO₃ flows in the area (Canals and Ballesteros, 1997).

Moreover, during mid January 2011 there was a sharp increment in the CaCO₃ concentration (70%) coinciding with the Chl-*a* concentration maximum (Fig. 2). Although coccolithophore blooms may trigger rapid increments in CaCO₃ and OC (Malinverno et al., 2009), and have been identified as one of the most representative groups during the early stages of the phytoplankton bloom in the Balearic Sea (Valencia-Vila et al., 2015), the observed CaCO₃ peak was not associated with an increment in the OC fraction. Furthermore, during this CaCO₃ increment, the OC/N ratio (8) (Fig. 2) was too high to derive from a phytoplankton bloom (Middelburg and Nieuwenhuize, 1998). Thus, it would appear that the CaCO₃ registered during January 2011 likely derived from resuspension processes also.

During T1 and T2, the OC and biogenic opal fractions were the smallest ones (Fig. 2). Both fractions presented smaller values than those reported in the southern and northern slopes of the Balearic Archipelago where pelagic inputs are the major contributors to the TMF (Pasqual et al., 2015). This suggests that the pelagic inputs in the study area are comparatively lower. However, they can also be diluted by continental shelf and slope resuspension inputs that are funnelled into the Menorca canyon. This would agree with patterns observed in other Mediterranean canyons where particle fluxes within the canyon showed smaller OC and opal fractions than those collected in the adjacent slope (Puig and Palanques, 1998; Lopez-Fernandez et al., 2013b). The OC and biogenic opal in the present study showed similar percentages to those observed in other Mediterranean submarine canyons under higher pelagic production regimes (Table 4; Bonnin et al., 2008; Pasqual et al., 2013) providing further support to this hypothesis.

During mid spring and summer of 2011 and 2012, we observed a reduction in the OC fraction (Fig. 2). In this period the water column in the Balearic Archipelago starts stratifying (Fernández de Puellas et al., 2007), as in most areas of the western Mediterranean (Estrada, 1996). This stratification leads to a nutrient depletion in the euphotic zone (Estrada, 1996) causing a reduction in primary production (Marty et al., 2002) and pelagic OC fluxes that characterize the Mediterranean seasonal rhythm in trophic activities (Coma et al., 2000). However, despite this reduction in the OC fraction most spring and summer samples presented low OC/N ratios (5–6.5) (Fig. 2), suggesting that poor OC pelagic particle inputs were higher than those from resuspension. This would agree with the fact that during this period very few significant wave height events were registered (Table 3).

The highest opal percentages detected during spring and early summer did not coincide with the surface Chl-*a* maximum (Fig. 2). This is in contrast with previous studies in Mediterranean submarine canyons (Martín et al., 2006; Pasqual et al., 2010) and slopes (Sanchez-Vidal et al., 2005; Stavrakakis et al., 2013) which have reported simultaneous increments in OC and opal associated with the

winter–spring phytoplankton bloom. Thus, the low opal concentrations registered in the present study during the winter surface Chl-*a* maximum (Fig. 2) suggest that other phytoplankton groups may have overshadowed siliceous phytoplankton. This would agree with Estrada et al. (1999) who observed that during the winter spring bloom, phytoplankton biomass was not associated with diatom dominance in the Balearic Sea. The weak relationship between surface Chl-*a* concentrations and late spring and early summer opal maximums (Fig. 2) may be explained by the development of a deep chlorophyll maximum (~60 m) closely related to the nutricline (Crombet et al., 2011). In other oligotrophic areas of the Mediterranean Sea it has been reported that under high-stratified conditions, diatoms can dominate the deep chlorophyll maximum (Crombet et al., 2011). The low OC/N ratio (5–6.5) observed in late spring and early summer also suggests that the opal maximums derived from a deep chlorophyll maximum (Fig. 2).

Maximum opal percentages registered during early May to late June 2011 were 47% lower than opal percentages registered during early May to late June 2012 (Fig. 2). During spring and early summer 2011 the study area was influenced by recent AW (Fig. 8), which is considered highly oligotrophic (García et al., 2005). Conversely, during spring and summer 2012 the study area was influenced by resident AW (Fig. 9), which has a higher H₄SiO₄ content than recent AW (Crombet et al., 2011). These higher H₄SiO₄ concentrations in resident AW likely derive from more frequent river discharges than in recent AW, which has less residence time in the Mediterranean (Ludwig et al., 2009). In this regard, we hypothesize that higher opal fluxes observed during T2 could result from higher H₄SiO₄ availability, which could trigger the deep chlorophyll maximums and support larger siliceous phytoplankton populations.

5.4. Macroscopic components

Throughout both sampling intervals fecal pellet fluxes (Fig. 3g) presented several peaks, but only one peak coincided with the winter spring bloom (February 2011) (Fig. 5). This temporal pattern contrasts with zooplankton dynamics in the Balearic archipelago (Cartes et al., 2008) and long-term fecal pellet patterns in other areas of the western Mediterranean that showed a clear relationship between the winter–spring phytoplankton bloom and fecal pellet maximums (Fowler et al., 1991). During T2, when resident AW strongly influenced the southern slope of the archipelago (Fig. 9), fecal pellet fluxes were one order of magnitude higher than during T1 (Fig. 4). In the Balearic Archipelago, higher zooplankton abundances have been observed under the influence of resident AW (Fernández de Puellas et al., 2007). It has been suggested that resident AW may be able to sustain high zooplankton abundances since it facilitates higher “fertility” conditions than recent AW (López-Jurado, 2002). Furthermore, fecal pellets may induce rapid vertical transports enhancing biogenic component fluxes (Monaco et al., 1990; Stone and Steinberg, 2016). However, this does not seem to be the case in the Menorca canyon, since fecal pellet fluxes were not significantly correlated to any biogenic component (CaCO₃, $p = .51$ and $p = .34$ T1 and T2, respectively; OC, $p = .32$ and $p = .34$ T1 and T2, respectively; and opal fluxes $p = .06$ and $p = .07$ T1 and T2, respectively) suggesting that fecal pellets represented a low contribution to biogenic fluxes.

The fluxes of *P. oceanica* fragments (Fig. 4e and f) presented high variability throughout both sampling periods and were not significantly correlated with TMF (Figs. 5 and 6). During the T1 fluxes of *P. oceanica*, detritus remained quite stable and could not be related to any environmental pattern. Conversely, during T2, fluxes were more variable and there seemed to be a relationship between relatively high *P. oceanica* detritus fluxes and significant wave high events (Fig. 5 and Table 3). Indeed, inner shelf resuspension processes have been identified as a major source of macrophyte and sea grass detritus in deeper environments (Britton-Simmons et al., 2012). In North Pacific canyons, macrophyte and seagrass detritus have shown to be a major carbon

source, accounting for 20–83% of the particulate organic carbon (Harrold et al., 1998). However, *P. oceanica* detritus did not significantly correlated to the bulk OC flux during neither of the study periods T1 or T2 ($p = .33$ and $p = .35$, respectively). Despite this lack of correlation, *P. oceanica* detritus cannot be ruled out as a major carbon sink in deep Mediterranean environments due to its refractory nature (Danovaro et al., 1994) and high carbon contents (Romero et al., 1992). In this regard, peaks in *P. oceanica* detritus registered during mid December 2011 and early February 2012 coincided with high OC/N ratio (9–9.5) (Figs. 5 and 2). However, it should be mentioned that very small, reworked fragments represented the *P. oceanica* detritus fraction and this material should behave as a particle lighter than CaCO_3 or lithogenic sediment of the same size. This implies a more complicated relationship between transport mechanisms related to the coincidence of *P. oceanica* fragments at the beach and shallow coastal areas, and resuspension and downslope transport mechanisms. In any case, the presence of this component cannot be explained with the data available.

Benthic and pelagic foraminifera presented similar trends during both sampling periods, with poor correlation with the TMF pattern (Fig. 5 and Supplementary Material 2). During early spring to late summer 2011 there was a substantial increment in the fluxes of both foraminifera groups (Fig. 5). Coinciding with this increment, we observed an increase in turbidity, suggesting that these peaks in foraminifera fluxes derive from resuspension processes (Figs. 5 and 7). This mechanism seems feasible since pelagic foraminifera reaches its maximum concentrations in the water column during the winter months (Pujol and Grazzini, 1995).

In T2, the highest pelagic and benthic foraminifera fluxes were simultaneously registered during winter. Pujol and Grazzini (1995) reported that the highest densities of pelagic foraminifera in the Mediterranean Sea occurred during winter, which seem to be also observed in our sediment trap collections. Benthic foraminifera fluxes coincided with *P. oceanica* detritus peaks and significant wave height events suggesting that they most likely derive from resuspension processes (Table 3).

The lack of correlation between benthic and pelagic foraminifera and CaCO_3 fluxes ($p < .05$ both pelagic and benthic) suggests that the contribution of foraminifera to the CaCO_3 fluxes is so small that is diluted by other CaCO_3 sources (e.g. sediment). During both sampling periods, microplastic fibers (Fig. 3h) were found in all samples. Future research should quantify the amount of carbon that these artificial polymers introduce into the carbon flux and how they possibly bias the budget of naturally produced OC carbon.

6. Conclusions

Particle fluxes collected in the Menorca canyon head were comparatively low in the Mediterranean context, reflecting the sediment starved and oligotrophic nature of the study area. Significant inter-annual differences in the TMF and the main geochemical components were not found. There was not a clear parameter controlling the temporal variation and composition of the TMF; however, physical processes e.g., resuspension, seemed to be more important than biological production in the control of the magnitude and composition of the TMF in this insular canyon. The presence of resident AW seems to have a positive effect on the fecal pellet fluxes. In spite of the small TMF and its main constituents, it seems that local benthic communities find enough biogenic material to thrive on the Menorca canyon's head and adjacent continental shelf and slope.

Acknowledgements

The authors thank the crew of the R/V *García del Cid*, Javier Romero and Aurora M. Ricart for their help in the identification of *P. oceanica* detritus, Claudio Lo Iacono for providing the study area figure and

Silvia De Diago and Neus Maestro for their technical support. This work was funded by the European project LIFE + INDEMARES “Inventario y designación de la red Natura 2000 en áreas marinas del estado español” (LIFE07/NAT/E/000732).

Appendix A. Supplementary material

Supplementary data associated with this article can be found, in the online version, at <http://dx.doi.org/10.1016/j.pocan.2017.11.005>.

References

- Acosta, J., Canals, M., Herranz, P., Serra, J., Sanz, J.L., Casas, A., Mateu, G., Clafat, A., Casamor, E., San Gil, C., 1991. Morfología y Ambientales de la Cabecera del Cañon de Menorca (Morphology and Sedimentary Environments of the Menorca Canyon Head). Map (1:25,000) and Text (Spanish and English) Instituto Español de Oceanografía, Madrid (1991).
- Acosta, J., Muñoz, A., Herranz, P., Palomo, C., Ballesteros, M., Vaquero, M., Uchupi, E., 2001. Geodynamics of the Emile Baudot escarpment and the Balearic Promontory, western Mediterranean. *Mar. Pet. Geol.* 18, 349–369.
- Acosta, J., Canals, M., López-Martínez, J., Muñoz, A., Herranz, P., Urgeles, R., Palomo, C., Casamor, J.L., 2002. The Balearic Promontory geomorphology (western Mediterranean): morphostructure and active processes. *Geomorphology* 49, 177–204. [http://dx.doi.org/10.1016/S0169-555X\(02\)00168-X](http://dx.doi.org/10.1016/S0169-555X(02)00168-X).
- Alonso, B., Guillén, J., Canals, M., Serra, J., Acosta, J., Herranza, P., Sanz, J.L., Calafat, A., Catafau, E., 1988. Los sedimentos de la plataforma continental balear. *Acta Geológica Hispánica* 23, 185–196.
- Amores, A., Monserrat, S., Marcos, M., 2013. Vertical structure and temporal evolution of an anticyclonic eddy in the Balearic Sea (western Mediterranean). *J. Geophys. Res.: Oceans* 118, 2097–2106. <http://dx.doi.org/10.1002/jgrc.20150>.
- Amores, A., Monserrat, S., 2014. Hydrodynamic comparison between the north and south of Mallorca Island. *J. Mar. Syst.* 138, 40–50. <http://dx.doi.org/10.1016/j.jmarsys.2014.01.005>.
- Amores, A., Rueda, L., Monserrat, S., Guijarro, B., Pasqual, C., Massutí, E., 2014. Influence of the hydrodynamic conditions on the accessibility of *Aristeus antennatus* and other demersal species to the deep water trawl fishery off the Balearic Islands (western Mediterranean). *J. Mar. Syst.* 138, 203–210. <http://dx.doi.org/10.1016/j.jmarsys.2013.11.014>.
- Anderson, M.J., 2001. A new method for non-parametric multivariate analysis of variance. *Austral Ecol.* 26, 32–46.
- Balbín, R., Flexas, M.M., López-Jurado, J.L., Peña, M., Amores, A., Alemany, F., 2012. Vertical velocities and biological consequences at a front detected at the Balearic Sea. *Cont. Shelf Res.* 47, 28–41. <http://dx.doi.org/10.1016/j.csr.2012.06.008>.
- Balbín, R., López-Jurado, J.L., Flexas, M.M., Reglero, P., Vélez-Velchí, P., González-Pola, C., Rodríguez, J.M., García, A., Alemany, F., 2014. Interannual variability of the early summer circulation around the Balearic Islands: driving factors and potential effects on the marine ecosystem. *J. Mar. Syst.* 138, 70–81. <http://dx.doi.org/10.1016/j.jmarsys.2013.07.004>.
- Bonnin, J., Heussner, S., Calafat, A., Fabres, J., Palanques, A., Durrieu de Madron, X., Canals, M., Puig, P., Avril, J., Delsaut, N., 2008. Comparison of horizontal and downward particle fluxes across canyons of the Gulf of Lions (NW Mediterranean): meteorological and hydrodynamical forcing. *Cont. Shelf Res.* 28, 1957–1970. <http://dx.doi.org/10.1016/j.csr.2008.06.004>.
- Bosc, E., Bricaud, A., Antoine, D., 2004. Seasonal and interannual variability in algal biomass and primary production in the Mediterranean Sea, as derived from 4 years of SeaWiFS observations. *Global Biogeochem. Cycles* 18, 1–17. <http://dx.doi.org/10.1029/2003GB002034>.
- Britton-Simmons, K.H., Rhoades, A.L., Pacunski, R.E., Galloway, A.W.E., Lowe, A.T., Sosik, A.E., Dethier, M.N., Duggins, D.O., 2012. Habitat and bathymetry influence the landscape-scale distribution and abundance of drift macrophytes and associated invertebrates. *Limnol. Oceanogr.* 57, 176–184. <http://dx.doi.org/10.4319/lo.2012.57.1.0176>.
- Chambers, J.M., 1992. Linear models. In: Hastie, T.J., Chambers, J.M. (Eds.), *Statistical Models*. S. Wadsworth & Brooks, Cole, Pacific Grove, California (chapter 4).
- Canals, M., Ballesteros, E., 1997. Production of carbonate particles by phyto-benthic communities on the Mallorca-Menorca shelf, northwestern Mediterranean Sea. *Deep Sea Res. Part II* 44, 611–629. [http://dx.doi.org/10.1016/S0967-0645\(96\)00095-1](http://dx.doi.org/10.1016/S0967-0645(96)00095-1).
- Cartes, J.E., Madurell, T., Fanelli, E., López-Jurado, J.L., 2008. Dynamics of supra-benthos-zooplankton communities around the Balearic Islands (western Mediterranean): influence of environmental variables and effects on the biological cycle of *Aristeus antennatus*. *J. Mar. Syst.* 71, 316–335. <http://dx.doi.org/10.1016/j.jmarsys.2006.11.013>.
- Casalbore, D., Falese, F., Martorelli, E., Romagnoli, C., Chiocci, F.L., 2016. Submarine depositional terraces in the Tyrrhenian Sea as a proxy for paleo-sea level reconstruction: problems and perspective. *Quatern. Int.* 439, 169–180.
- Colom, G., 1974. Foraminíferos ibéricos. Introducción al estudio de las especies bentónicas recientes. Investigación Pesquera, Consejo Superior de Investigaciones Científicas, vol. 38. Patrono Juan de la Cierva, Barcelona.
- Coma, R., Ribes, M., Gili, J.M., Zabala, M., 2000. Seasonality in coastal benthic ecosystems. *Trends Ecol. Evol.* 15, 448–453.
- Courp, T., Monaco, A., 1990. Sediment and accumulation on the continental margin of the Gulf of Lions: sedimentary budget. *Cont. Shelf Res.* 10, 1063–1087.

- Crombet, Y., Leblanc, K., Quéguiner, B., Moutin, T., Rimmelin, P., Ras, J., Claustre, H., Leblond, N., Oriol, L., Pujo-Pay, M., 2011. Deep silicon maxima in the stratified oligotrophic Mediterranean Sea. *Biogeosciences* 8, 459–475. <http://dx.doi.org/10.5194/bg-8-459-2011>.
- Danovaro, R., Fabiano, M., Boyer, M., 1994. Seasonal changes of benthic bacteria in a seagrass bed (*Posidonia oceanica*) of the Ligurian Sea in relation to origin, composition and fate of the sediment organic matter. *Mar. Biol.* 119, 489–500. <http://dx.doi.org/10.1007/BF00354310>.
- Danovaro, R., Dinet, A., Duineveld, G., Tselepidis, A., 1999. Benthic response to particulate fluxes in different trophic environments: a comparison between the Gulf of Lions-Catalan Sea (western-Mediterranean) and the Cretan Sea (eastern-Mediterranean). *Prog. Oceanogr.* 44, 287–312. [http://dx.doi.org/10.1016/S0079-6611\(99\)00030-0](http://dx.doi.org/10.1016/S0079-6611(99)00030-0).
- DeMaster, D., 1981. The supply and accumulation of silica in the marine environment. *Geochim. Cosmochim. Acta* 45, 1715–1732.
- Durrieu de Madron, X., Radakovitch, O., Heussner, S., Loye-Pilot, M.D., Monaco, A., 1999. Role of the climatological and current variability on shelf-slope exchanges of particulate matter: evidence from the Rhone continental margin (NW Mediterranean). *Deep Sea Res. Part I* 46, 1513–1538. [http://dx.doi.org/10.1016/S0967-0637\(99\)00015-1](http://dx.doi.org/10.1016/S0967-0637(99)00015-1).
- Durrieu de Madron, X., Ramondenc, S., Berline, L., Houpert, L., Bosse, A., Martini, S., Guidi, L., Conan, P., Curtil, C., Delsaut, N., Kunesch, S., Ghiglione, J.F., Marsaleix, P., Pujo-Pay, M., Séverin, T., Testor, P., Tamburini, C., 2017. J. Geophys. Res.: Oceans 122, 2291–2318. <http://dx.doi.org/10.1002/2016/JC012062>.
- Estrada, M., 1996. Primary production in the northwestern Mediterranean. *Sci. Mar.* 60, 55–64.
- Estrada, M., Varela, R.A., Salat, J., Cruzado, A., 1999. Spatio-temporal variability of the winter phytoplankton distribution across the Catalan and North Balearic fronts (NW Mediterranean). *J. Plankton Res.* 21, 1–20.
- Fabrés, J., Calafat, A., Sanchez-Vidal, A., Canals, M., Heussner, S., 2002. Composition and spatial variability of particle fluxes in the Western Alborán Gyre, Mediterranean Sea. *J. Mar. Syst.* 33–34, 431–456.
- Favalli, M., Karátson, D., Mazzuoli, R., Pareschi, M.T., Ventura, G., 2005. Volcanic geomorphology and tectonics of the Aeolian archipelago (Southern Italy) based on integrated DEM data. *Bull. Bolcanol.* 68, 157–170.
- Fernández de Puellas, M.L., Alemany, F., Jansá, J., 2007. Zooplankton time-series in the Balearic Sea (Western Mediterranean): variability during the decade 1994–2003. *Prog. Oceanogr.* 74, 329–354. <http://dx.doi.org/10.1016/j.pocean.2007.04.009>.
- Fowler, S.W., Small, L.F., Larosa, J., 1991. Seasonal particulate carbon flux in the coastal northwestern mediterranean-sea, and the role of zooplankton fecal matter. *Oceanol. Acta* 14, 77–85.
- García, A., Alemany, F., Velez-Belchí, P., López Jurado, J.L., Cortés, D., de la Serna, J.M., González Pola, C., Rodríguez, J.M., Jnasá, J., Ramírez, T., 2005. Characterization of the bluefin tuna spawning habitat off the Balearic Archipelago in relation to key hydrographic features and associated environmental. *ICCAT Collective Volume of Scientific Papers* 58, 535–549.
- García Pérez, A., 2005. Estadística aplicada: conceptos básicos. UNED Editorial, Madrid.
- Grinyó, J., 2016. Ecological study of benthic communities in the continental shelf and upper slope in the Menorca Channel (North Western Mediterranean Sea). (Ph.D. thesis). <http://dx.doi.org/10.13140/RG.2.2.24275.78885>.
- Guillén, J., Bourrin, F., Palanques, A., Durrieu de Madron, X., Puig, P., Buscail, R., 2006. Sediment dynamics during wet and dry storm events on the Têt inner shelf (SW Gulf of Lions). *Mar. Geol.* 234, 129–142. <http://dx.doi.org/10.1016/j.margeo.2006.09.018>.
- Hammer, T., Harper, D.A.T., Ryan, P.D., 2001. PAST: paleontological statistics software package for education and data analysis. *Palaentologia Electron.* 4, 1–9.
- Harris, P.T., Whiteway, T., 2011. Global distribution of large submarine canyons: geomorphic differences between active and passive continental margins. *Mar. Geol.* 285, 69–86. <http://dx.doi.org/10.1016/j.margeo.2011.05.008>.
- Harrold, C., Light, K., Lisin, S., 1998. Organic enrichment of submarine-canyon and continental-shelf benthic communities by macroalgal drift imported from nearshore kelp forests. *Limnol. Oceanogr.* 43, 669–678.
- Hasiotis, T., Papatheodorou, G., Ferentinos, G., 2007. Sediment stability conditions Wes of Milos Island, Weste Hellenic Bolcanic Arc. In: Lykousis, V., Sakellariou, D., Locat, J. (Eds.), *Submarine Mass Movements and Their Consequences*. Springer, Dordrecht, Netherlands, pp. 317–324.
- Heussner, S., Ratti, C., Carbonne, J., 1990. The PPS 3 time series sediment traps and the trap sample processing techniques used during the ECOMARGE experiment. *Cont. Shelf Res.* 10, 943–958.
- Heussner, S., Durrieu de Madron, X., Calafat, A., Canals, M., Carbonne, J., Delsaut, N., Saragoni, G., 2006. Spatial and temporal variability of downward particle fluxes on a continental slope: lessons from an 8-yr experiment in the Gulf of Lions (NW Mediterranean). *Mar. Geol.* 234, 63–92. <http://dx.doi.org/10.1016/j.margeo.2006.09.003>.
- Katz, T., Ginat, H., Eyal, G., Steiner, S., Braun, Y., Shalev, S., Goodman-Tchernov, G.N., 2015. Desert flash floods form hypercynical flows in the coral-rich Gulf of Aqab, Red Sea. *Earth Planet. Sci. Lett.* 417, 87–98.
- Khripounoff, A., Vangriesheim, A., Babonneau, N., Crassous, P., Dennielou, B., Savoye, B., 2003. Direct observation of intense turbidity current activity in the Zaire submarine valley at 4000 m water depth. *Mar. Geol.* 194, 151–158. [http://dx.doi.org/10.1016/S0025-3227\(02\)00677-1](http://dx.doi.org/10.1016/S0025-3227(02)00677-1).
- Khripounoff, A., Crassous, P., Lo Bue, N., Dennielou, B., Jacinto, R.S., 2012. Different types of sediment gravity flows detected in the Var submarine canyon (northwestern Mediterranean Sea). *Prog. Oceanogr.* 106, 138–153. <http://dx.doi.org/10.1016/j.pocean.2012.09.001>.
- Kineke, G.C., Woolfe, K.J., Kuehl, S.A., Milliman, J.D., Dellapenna, T.M., Purdon, R.G., 2000. Sediment export from the Sepik River, Papua New Guinea: evidence for a divergent sediment plume. *Cont. Shelf Res.* 20, 2239–2266. [http://dx.doi.org/10.1016/S0278-4343\(00\)00069-8](http://dx.doi.org/10.1016/S0278-4343(00)00069-8).
- Liu, J.T., Liu, K.J., Huang, J.C., 2002. The effect of a submarine canyon on the river sediment dispersal and inner shelf sediment movements in southern Taiwan. *Mar. Geol.* 181, 357–386. [http://dx.doi.org/10.1016/S0025-3227\(01\)00219-5](http://dx.doi.org/10.1016/S0025-3227(01)00219-5).
- Lo Iacono, C., Urgeles, R., Polizzi, S., Grinyó, J., Druet, M., Agate, M., Gili, J.M., Acosta, J., 2014. Submarine mass movements and their consequences. In: *Submarine Mass Movements Along a Sediment Starved Margin: The Menorca Channel (Balearic Islands-Western Mediterranean)*, pp. 329–338. <http://dx.doi.org/10.1007/978-1-4020-6512-5>.
- Lopez-Fernandez, P., Bianchelli, S., Pusceddu, A., Calafat, A., Danovaro, R., Canals, M., 2013a. Bioavailable compounds in sinking particulate organic matter, Blanes Canyon, NW Mediterranean Sea: effects of a large storm and sea surface biological processes. *Prog. Oceanogr.* 118, 108–121. <http://dx.doi.org/10.1016/j.pocean.2013.07.022>.
- Lopez-Fernandez, P., Calafat, A., Sanchez-Vidal, A., Canals, M., Flexas, M.M., Cateura, J., Company, J.B., 2013b. Multiple drivers of particle fluxes in the Blanes submarine canyon and southern open slope: results of a year round experiment. *Prog. Oceanogr.* 118, 95–107. <http://dx.doi.org/10.1016/j.pocean.2013.07.029>.
- López-Jurado, J.L., 2002. Interannual variability in waters of the Balearic Islands. In: Briand, F., (Ed.), *Tracking Long-Term Hydrological Change in the Mediterranean Sea*. CIESM Workshop series. vol. 16, pp. 33–36.
- Ludwig, W., Dumont, E., Meybeck, M., Heussner, S., 2009. River discharges of water and nutrients to the Mediterranean and Black Sea: major drivers for ecosystem changes during past and future decades? *Prog. Oceanogr.* 80, 199–217.
- Malinverno, E., Triantaphyllou, M.V., Stavrakakis, S., Ziveri, P., Lykousis, V., 2009. Seasonal and spatial variability of coccolithophore export production at the South-Western margin of Crete (Eastern Mediterranean). *Mar. Micropaleontol.* 71, 131–147. <http://dx.doi.org/10.1016/j.marmicro.2009.02.002>.
- Martín, J., Palanques, A., Puig, P., 2006. Composition and variability of downward particulate matter fluxes in the Palamós submarine canyon (NW Mediterranean). *J. Mar. Syst.* 60, 75–97. <http://dx.doi.org/10.1016/j.jmarsys.2005.09.010>.
- Martín, J., Palanques, A., Vitorino, J., Oliveira, A., de Stigter, H.C., 2011. Near-bottom particulate matter dynamics in the Nazaré submarine canyon under calm and stormy conditions. *Deep Sea Res. II: Top. Stud. Oceanogr.* 58, 2388–2400. <http://dx.doi.org/10.1016/j.dsr2.2011.04.004>.
- Marty, J.C., Chiavérini, J., Pizay, M.D., Avril, B., 2002. Seasonal and interannual dynamics of nutrients and phytoplankton pigments in the western Mediterranean Sea at the DYFAMED time-series station (1991–1999). *Deep Sea Res. Part II* 49, 1965–1985. [http://dx.doi.org/10.1016/S0967-0645\(02\)00022-X](http://dx.doi.org/10.1016/S0967-0645(02)00022-X).
- Middelburg, J.J., Nieuwenhuize, J., 1998. Carbon and nitrogen stable isotopes in suspended matter and sediments from the Schelde Estuary. *Mar. Chem.* 60, 217–225. [http://dx.doi.org/10.1016/S0304-4203\(97\)00104-7](http://dx.doi.org/10.1016/S0304-4203(97)00104-7).
- Millot, C., 1987. Circulation in the Western Mediterranean Sea. *Oceanol. Acta* 10, 143–148.
- Miserocchi, S., Faganeli, J., Balboni, V., Heussner, S., Monaco, A., Kerherve, P., 1999. Characteristics and sources of the settling particulate organic matter in the South Adriatic basin. *Org. Geochem.* 30, 411–421. [http://dx.doi.org/10.1016/S0146-6380\(99\)00026-1](http://dx.doi.org/10.1016/S0146-6380(99)00026-1).
- Monaco, A., Courp, T., Heussner, S., Carbonne, J., Fowler, S.W., Daniaux, B., 1990. Seasonality and composition of particulate fluxes during ECOMARGE—I, western Gulf of Lions. *Cont. Shelf Res.* 10, 9–11. [http://dx.doi.org/10.1016/0278-4343\(90\)90070-3](http://dx.doi.org/10.1016/0278-4343(90)90070-3).
- Moranta, J., Barberá, C., Druet, M., Zaragoza, N., 2014. Caracterización ecológica de la plataforma continental (50–100 m) del canal de Menorca. Informe final área LIFE + INDEMARCA (LIFE07/NAT/E/000732). Institutut Espanol de Oceanografía-Centro Oceanográfico de Baleares (Palma). Fundación Biodiversidad, Palma, Coordinación, 504 p.
- Mortlock, R.A., Froelich, P.N., 1989. A simple method for the rapid determination of biogenic opal in marine pelagic sediments. *Deep Sea Res. Part A. Oceanogr. Res. Papers* 36, 1415–1426.
- Mullenbach, B.L., Nittrouer, C.A., Puig, P., Orange, D.L., 2004. Sediment deposition in a modern submarine canyon: Eel Canyon, northern California. *Mar. Geol.* 211, 101–119. <http://dx.doi.org/10.1016/j.margeo.2004.07.003>.
- Obrador, A., Pomar, L., Taberner, C., 1992. Late Miocene breccia of Menorca (Balearic Islands): a basis for the interpretation of a Neogene ramp deposit. *Sed. Geol.* 79, 203–233.
- O'Brien, M.C., Melling, H., Pedersen, T.F., Macdonald, R.W., 2013. The Role of eddies on particle flux in the Canada basin of the Arctic Ocean. *Deep-Sea Res. Part I: Oceanogr. Res. Papers* 171, 1–20. <http://dx.doi.org/10.1016/j.dsr.2012.10.004>.
- Palanques, A., El Khatab, M., Puig, P., Masque, P., Sa, J.A., Isla, E., 2005. Downward particle fluxes in the Guadiaro submarine canyon depositional system (north-western Alboran Sea), a river flood dominated system. *Mar. Geol.* 220, 23–40. <http://dx.doi.org/10.1016/j.margeo.2005.07.004>.
- Palanques, A., Martín, J., Puig, P., Guillén, J., Company, J.B., Sardá, F., 2006. Evidence of sediment gravity flows induced by trawling in the Palamós (Fonera) submarine canyon (northwestern Mediterranean). *Deep Sea Res. Part I* 53, 201–214.
- Pasqual, C., Sanchez-Vidal, A., Zúñiga, D., Calafat, A., Canals, M., Durrieu de Madron, X., Puig, P., Heussner, S., Palanques, A., Delsaut, N., 2010. Flux and composition of settling particles across the continental margin of the Gulf of Lion: the role of dense shelf water cascading. *Biogeosciences* 7, 217–231.
- Pasqual, C., Goñi, M.A., Tesi, T., Sanchez-Vidal, A., Calafat, A., Canals, M., 2013. Composition and provenance of terrigenous organic matter transported along submarine canyons in the Gulf of Lion (NW Mediterranean Sea). *Prog. Oceanogr.* 118, 81–94. <http://dx.doi.org/10.1016/j.pocean.2013.07.013>.
- Pasqual, C., Amores, A., Flexas, M.M., Monserrat, S., Calafat, A., 2014. Environmental

- factors controlling particulate mass fluxes on the Mallorca continental slope (Western Mediterranean Sea). *J. Mar. Syst.* 138, 63–69. <http://dx.doi.org/10.1016/j.jmarsys.2014.05.008>.
- Pasqual, C., Calafat, A., Lopez-Fernandez, P., Pusceddu, A., 2015. Organic carbon inputs to the sea bottom of the Mallorca continental slope. *J. Mar. Syst.* 148, 142–151. <http://dx.doi.org/10.1016/j.jmarsys.2015.02.006>.
- Puig, P., Palanques, A., 1998. Temporal variability and composition of settling particle fluxes on the Barcelona continental margin (Northwestern Mediterranean). *J. Mar. Res.* 56, 639–654. <http://dx.doi.org/10.1357/002224098765213612>.
- Puig, P., Ogston, A.S., Mullenbach, B.L., Nittrouer, C.A., Parsons, J.D., Sternberg, R.W., 2004. Storm-induced sediment gravity flows at the head of the Eel submarine canyon, northern California margin. *J. Geophys. Res.: Oceans* 109, 1–10. <http://dx.doi.org/10.1029/2003JC001918>.
- Puig, P., Palanques, A., Martín, J., Ribó, M., Guillén, J., 2014. Benthic storms in the north-western Mediterranean continental rise caused by deep dense water formation. 2nd Deep-Water Circulation Congress 27–28.
- Pujol, C., Grazzini, C.V., 1995. Distribution patterns of live planktic foraminifers as related to regional hydrography and productive systems of the Mediterranean Sea. *Mar. Micropaleontol.* 25, 187–217. [http://dx.doi.org/10.1016/0377-8398\(95\)00002-1](http://dx.doi.org/10.1016/0377-8398(95)00002-1).
- Quaresma, L.S., Vitorino, J., Oliveira, A., Da Silva, J., 2007. Evidence of sediment re-suspension by nonlinear internal waves on the western Portuguese mid-shelf. *Mar. Geol.* 246, 123–143.
- R Core Team, 2014. R: A Language and Environment for Statistical Computing. R Foundation for Statistical Computing, Vienna, Austria. <http://www.R-project.org>.
- Ribó, M., Puig, P., Muñoz, A., Lo Iacono, C., Masqué, P., Palanques, A., Acosta, J., Guillén, J., Ballesteros, M.G., 2016. Morphobathymetric analysis of the large fine-grained sediment waves over the Gulf of Valencia continental slope (NW Mediterranean). *Geomorphology* 253, 22–37.
- Rigual-Hernández, A.S., Bárcena, M.A., Jordan, R.W., Sierro, F.J., Flores, J.A., Meier, K.J.S., Beaufort, L., Heussner, S., 2013. Diatom fluxes in the NW Mediterranean: evidence from a 12-year sediment trap record and surficial sediments. *J. Plankton Res.* 35, 1109–1125. <http://dx.doi.org/10.1093/plankt/fbt055>.
- Romagnoli, C., Kokelaar, P., Casalbone, D., Chiocci, F.L., 2009. Lateral collapses and active sedimentary processes on the northwestern flank of Stromboli volcano, Italy. *Mar. Geol.* 265, 101–119.
- Romero, J., Pergent, G., Pergent-Martini, C., Mateo, M., Regnier, C., 1992. The Detritic Compartment in a *Posidonia oceanica* Meadow: litter features, decomposition rates, and mineral stocks. *Mar. Ecol.* 13, 69–83. <http://dx.doi.org/10.1111/j.1439-0485.1992.tb00341.x>.
- Ross, C.B., Gardner, W.D., Richardson, M.J., Asper, V.L., 2009. Currents and sediment transport in the Mississippi Canyon and effects of Hurricane Georges. *Cont. Shelf Res.* 29, 1384–1396. <http://dx.doi.org/10.1016/j.csr.2009.03.002>.
- Sakellariou, D., Kourkoumelis, D., Rosakis, G., Goergiou, P., Panagiotopoulos, I., Morfisi, I., 2015. Deep-water geo-archaeological research along the POSEIDON pipeline route, Ionian Sea. 11th Panhellenic Symposium on Oceanography and Fisheries. Mytilene, Lesbos Island, Greece, pp. 1005–1008.
- Sanchez-Cabeza, J.A., Masqué, P., Ani-Ragolta, I., Merino, J., Frignani, M., Alvisi, F., Palanques, A., Puig, P., 1999. Sediment accumulation rates in the southern Barcelona continental margin (NW Mediterranean Sea) derived from 210P and 137Cs chronology. *Prog. Oceanogr.* 44, 313–332. [http://dx.doi.org/10.1016/S0079-6611\(99\)00031-2](http://dx.doi.org/10.1016/S0079-6611(99)00031-2).
- Sanchez-Vidal, A., Calafat, A., Canals, M., Frigola, J., Fabres, J., 2005. Particle fluxes and organic carbon balance across the Eastern Alboran Sea (SW Mediterranean Sea). *Cont. Shelf Res.* 25, 609–628. <http://dx.doi.org/10.1016/j.csr.2004.11.004>.
- Schmidt, S., Howa, H., Diallo, A., Martín, J., Cremer, M., Duros, P., Fontanier, C., Deflandre, B., Metzger, E., Mulder, T., 2014. Recent sediment transport and deposition in the Cap-Ferret Canyon, South-East margin of Bay of Biscay. *Deep-Sea Res. II* 104, 134–144.
- Shepard, F.P., Marshall, N.F., McLoughlin, P.A., 1974. Currents in submarine canyons. *Deep Sea Res. Oceanogr. Abstr.* 21, 691–706. [http://dx.doi.org/10.1016/0011-7471\(74\)90077-1](http://dx.doi.org/10.1016/0011-7471(74)90077-1).
- Stavrakakis, S., Chronis, G., Tselepidis, A., Heussner, S., Monaco, A., Abassi, A., 2000. Downward fluxes of settling particles in the deep Cretan Sea (NE Mediterranean). *Prog. Oceanogr.* 46, 217–240.
- Stavrakakis, S., Gogou, A., Krasakopoulou, E., Karageorgis, A.P., Kontoyiannis, H., Rousakis, G., Velaoras, D., 2013. Downward fluxes of sinking particulate matter in the deep Ionian Sea (NESTOR site), eastern Mediterranean: seasonal and interannual variability. *Biogeosciences* 10, 7235–7254. <http://dx.doi.org/10.5194/bg-10-7235-2013>.
- Stone, J.P., Steinberg, D.K., 2016. Salp contributions to vertical carbon flux in the Sargasso Sea. *Deep Sea Res. Part I* 113, 90–100. <http://dx.doi.org/10.1016/j.dsr.2016.04.007>.
- Syvitski, J.P., Morehead, M.D., 1999. Estimating river-sediment discharge to the ocean: application to the Eel margin, northern California. *Mar. Geol.* 154, 13–28. [http://dx.doi.org/10.1016/S0025-3227\(98\)00100-5](http://dx.doi.org/10.1016/S0025-3227(98)00100-5).
- Turchetto, M., Boldrin, A., Langone, L., Miserocchi, S., Tesi, T., Fogliani, F., 2007. Particle transport in the Bari Canyon (southern Adriatic Sea). *Mar. Geol.* 246, 231–247. <http://dx.doi.org/10.1016/j.margeo.2007.02.007>.
- Ulses, C., Estournel, C., Durrieu de Madron, X., Palanques, A., 2008. Suspended sediment transport in the Gulf of Lions (NW Mediterranean): impact of extreme storms and floods. *Cont. Shelf Res.* 28, 2048–2070. <http://dx.doi.org/10.1016/j.csr.2008.01.015>.
- Valencia-Vila, J., Fernández de Puelles, M.L., Jansá, J., Varela, M., 2015. Phytoplankton composition in a neritic area of the Balearic Sea (Western Mediterranean). *J. Mar. Biol. Assoc. United Kingdom* 96, 1–11. <http://dx.doi.org/10.1017/S0025315415001137>.
- Walsh, J.P., Nittrouer, C.A., 2003. Contrasting styles of off-shelf sediment accumulation in New Guinea. *Mar. Geol.* 196, 105–125.
- Walsh, J.P., Nittrouer, C.A., 2009. Understanding fine-grained river-sediment dispersal on continental margins. *Mar. Geol.* 263, 34–45.
- Xu, J.P., Noble, M., Eittrheim, S.L., Rosenfeld, L.K., Schwing, F.B., Pilskaln, C.H., 2002. Distribution and transport of suspended particulate matter in submarine canyons off Southern California. *Mar. Geol.* 181, 133–153.
- Zúñiga, D., Flexas, M.M., Sanchez-Vidal, A., Coenjaerts, J., Calafat, A., Jordà, G., García-Orellana, J., Puigdefàbregas, J., Canals, M., Espino, M., Sardà, F., Company, J.B., 2009. Particle fluxes dynamics in Blanes submarine canyon (Northwestern Mediterranean). *Prog. Oceanogr.* 82, 239–251. <http://dx.doi.org/10.1016/j.pcean.2009.07.002>.